A&A 378, 192–213 (2001)
DOI: 10.1051/0004-6361:20011130

Astronomy & Astrophysics

Radial mixing in protoplanetary accretion disks

I. Stationary disc models with annealing and carbon combustion

H.-P. Gail*

Institut für Theoretische Astrophysik, Universität Heidelberg, Tiergartenstraße 15, 69121 Heidelberg, Germany

Received 5 January 2001 / Accepted 8 August 2001

Abstract. The interplay between radial mixing process in protoplanetary accretion discs with processes leading to destruction or modification of the extinction properties of abundant dust species has significant consequences for the properties of the disk. This paper studies the consequences of annealing amorphous silicate dust at $T \approx 800\,\mathrm{K}$, of combustion of the carbon dust component at about $T \approx 1000\,\mathrm{K}$ and of mixing the products into cold outer disc regions out to 10 AU and beyond. A model calculation in the one-zone approximation for stationary Keplerian α-disks around a solar-like protostar is combined with a solution of the equations for annealing of silicate dust grains, for carbon dust oxidation, and a solution of the diffusion equations for radial mixing of the dust components in the disc by turbulent flows. It is shown that annealing of amorphous silicate dust reduces the mass extinction coefficient of the disc matter by more than an order of magnitude in the warm disc zone. Radial mixing of the freshly produced crystalline silicate dust into outer disc regions reduces the opacity of the disc material also in cold disc regions where annealing is not possible. Mixing of carbon dust free material from the zone of carbon combustion into outer disc regions also leads to a considerable reduction of the opacity of the disc material. Radial mixing processes then modify the dust composition of the outer disc regions and by means of the dependence of the disk properties (midplane temperature T_c, viscosity ν, ...) on the opacity also modify the structure and evolution of a protoplanetary disc. It is shown that turbulent mixing processes in the protoplanetary accretion disc of a Solar System like system during its evolution prior to the onset of the formation of planetary bodies carry material from inner disc regions $r < 1\,\mathrm{AU}$ outwards to at least 10...20 AU. This offers a simple explanation of the findings that a significant fraction of the cometary silicate dust grains are crystallised and that the matrix material of primitive meteorites contains thermally processed crystalline dust material.

Key words. accretion disks – molecular processes – solar system: formation

1. Introduction

Protostellar and protoplanetary accretion discs are usually believed to be in a state of vigorous turbulence during the early stages of their evolution. As is well known, if the carrier gas of a turbulent flow has a spatially inhomogeneous composition with respect to its main and/or tracer constituents, turbulence induces a spatial diffusion of the components which tends to eliminate any spatial concentration gradients. Morfill (1983) has pointed out that this process has important consequences for the composition of the material in a protoplanetary accretion disc if the turbulent part of the disc connects regions with widely different temperatures. Chemical and physical processes in warm and hot disc regions locally change the structure, properties and chemical composition of the various dust components which are part of the mixture forming the disc material. Turbulent mixing then carries such material into cold regions of the disc where it is mixed with freshly accreted material from the parent molecular cloud (Morfill 1983). Or dust components are vapourised in the hot parts of the disc and the vapours are mixed outwards by turbulent diffusion and recondense in cooler parts of the disc (Morfill 1983). Other important consequences of turbulence are, for instance, that grain coagulation is induced and vertical settling of grains to the midplane is suppressed as long as the gas is in a turbulent state.

Some consequences of turbulent transport processes for the composition of the disc material have extensively been discussed by Morfill & Völk (1984), Morfill (1985), and Morfill et al. (1985) and the basic equations describing the reaction, diffusion and transport processes have been worked out in great detail. Based on simple disc models it was shown by Morfill (1985) and Morfill et al. (1985) that nebular wide mixing of dust material between cold and

* e-mail: gail@ita.uni-heidelberg.de

warm disc zones is to be expected and explains some observed properties of primitive meteorites. Definite models for radial mixing in a protoplanetary disc, however, were not calculated.

Radial mixing of water vapour in the Solar Nebula has been studied by Stevenson & Lunine (1988) and of trace molecules by Stevenson (1990). Diffusion of deuterium in the Solar Nebula was studied by Drouart et al. (1999). These studies also indicate that diffusional mixing is important and has significant influence on the composition of the disc matter. Further the homogeneity of isotopic ratios of the heavy elements in the solar system is considered an indication that efficient (but not perfect) radial mixing took place in the early Solar Nebula.

A more direct indication for mixing of disc material comes from observations of dust emission from comets where an analysis of the silicate emission bands definitely shows that part of the silicate dust is crystalline. Hanner et al. (1994) discussed in their analysis of comet Mueller 1993a the origin of the crystalline dust component. As there is no indication for significant amounts of crystalline silicate dust to be present in the interstellar medium and in molecular clouds the crystalline dust is likely to originate within the Solar Nebula itself. It can result either from annealing of amorphous dust or by growth of crystalline grains from the gas phase. Both processes require elevated temperatures ($T \gtrsim 800\,\mathrm{K}$) which are encountered in the inner part of the solar nebula ($r \lesssim 1 \ldots 2\,\mathrm{AU}$), but not in the region beyond Jupiter where comets are thought to form. This indicates that some radial mixing took place between the inner and outer parts of the Solar Nebula. Wooden et al. (1999, 2000) discussed the structure of the silicate band in comet Hale–Bopp and showed that the cometary material contains a considerable fraction of crystalline silicates, probably with high magnesium content which is characteristic for chemical equilibrium condensates at high temperature (e.g. Saxena & Ericksson 1986). This indicates mixing of material from high temperature regions of the disc to the formation zone of cometary bodies. Another explanation may be that this material is of circumstellar origin from e.g. AGB stars, as is favoured by Wooden et al. (1999) which, however, immediately raises the question why no crystalline grains are seen in the ISM. Nuth (1999) and Nuth et al. (2000) interpreted the presence of crystalline material in comets as an indication of radial transport of matter from warm inner regions of a protostellar accretion disk where annealing of initially amorphous grains is possible to the cold outer zones of the disk. They point out, that possibly even an evolutionary sequence is seen in disks around pre main sequence A and B stars showing an increase of the amount of crystalline material present with age of the objects, which may result from progressive mixing.

The present paper extends the previous discussions of Duschl et al. (1996) and Gail (1998) of conversion of amorphous dust from the outer disc regions by annealing into crystalline dust in the inner dust regions and of carbon grain combustion. We consider radial turbulent mixing of dust in a protoplanetary accretion disc and combine this with a self consistent calculation of the structure of a stationary α-disc in the one-zone approximation. The main purpose of this model calculation is to determine the consequences of radial mixing of dust materials for the structure of a protoplanetary disk. This model calculation concentrates on two processes, which can be expected to be of considerable importance for the disc structure and evolution.

First we consider the annealing of amorphous dust from the outer disc region at a disc midplane temperature of roughly 800 K (Duschl et al. 1996; Gail 1998) and turbulent mixing of the resulting crystalline dust back into the outer disc zone. For silicates the transition from an amorphous state to a crystalline state is accompanied by a strong reduction of the mass extinction coefficient of at least a factor of ten. The mass extinction of the silicate dust component in regions of the disc that are warm enough for annealing to occur then is drastically lower than in the outer disc region where annealing is not possible. Mixing of annealed material outwards also reduces the dust opacity in a wide transition region. Since the structure of the disc strongly depends on the opacity of the disc material, annealing of silicate dust and mixing such material into outer regions will strongly modify the disc properties.

Secondly we consider the combustion of carbon dust in the inner disc region and the consequences of mixing the outburnt material back into outer regions. The dilution of disc material in the outer zones by mixing with carbon dust free material from the inner region reduces the carbon content in the mixed zones and, since carbon grains are one of the most important contributors to the opacity, considerably reduces the opacity of the disc material. This also changes the disk properties. The modifications of the gas phase chemistry resulting from mixing the burning products of carbon combustion into the cometary formation zone will be treated in a separate paper.

The model calculation in this paper considers an early phase of the evolution of a protoplanetary disc where mass infall from the surrounding molecular cloud has ceased and star formation has nearly come to completion and where the remaining disc slowly disappears by accretion onto the star. It is generally thought that planet formation in Solar System like systems starts at some instant during this phase of the disc evolution. All processes operating during this phase which result in the destruction or metamorphosis of any of the dust components in the disc material have direct implications for the composition of the planetesimals formed at the onset of the planetary formation process and left their footprints in the composition of cometary and meteoritic material. This makes the study of the chemical and mineralogical evolution of the disc material during this phase particular important.

This paper does not deal with time dependent models for protoplanetary accretion discs combined with radial mixing. The results for time dependent models will be published elsewhere (Wehrstedt & Gail, in preparation).

The plan of this paper is as follows: Sect. 2 discusses the reaction-transport-diffusion equation, Sect. 3 describes our model for calculating carbon combustion, Sect. 4 describes the model for calculating the annealing of amorphous dust, Sect. 5 gives details of our method of calculating disc models in the one-zone approximation, including the diffusion and transport processes. Section 6 presents the results. Section 7 presents some results for disc spectra. Section 8 gives our conclusions.

2. Mixing by diffusive transport

At least during the first million year after their formation protoplanetary accretion discs are unstable against convection throughout most parts of the disc ranging from the hot inner zone out to 20 AU or even more (see e.g. Ruden & Lin 1986 or D'Alessio et al. 1998). Additionally the disc is likely to be unstable against production of shear driven turbulence (Dubrulle 1993). For this reason, there exist turbulent flows in a protoplanetary accretion disc.

The origin of the viscous accretion which leads to conversion of gravitational energy into heat, which in turn drives the convection and the turbulence, is still not definitely known. We do not dwell on this part of the problem and the various mechanisms that have been proposed to be responsible for viscous accretion (cf. the reviews by Adams & Lin 1993; Papaloizou & Lin 1995; Lin & Papaloizou 1996) but simply rely on the fact that during the early evolution of a protoplanetary disc there is accretion with a rate of the order of $\dot{M} = 10^{-7}\,M_\odot\,\mathrm{yr}^{-1}$ (e.g. Hartmann 2000) which suffices completely to drive turbulent convection in the disc.

The random mixing of matter in such turbulent flows results in a diffusion like mixing of matter with a heterogeneous composition. We are specifically interested in the mixing of the various dust species existing in a protoplanetary accretion disk by this mechanism. The low particle density of each of the dust species allows us to treat the different components independently of each other and to consider simply the binary diffusion problem of a single dust species embedded in a carrier gas of much higher particle density. The diffusion equation for this problem is (Hirschfelder et al. 1964)

$$\frac{\partial n_i}{\partial t} + \frac{\partial}{\partial x_\mu} n_i v_\mu = \frac{\partial}{\partial x_\mu} n\, D_{ig} \frac{\partial}{\partial x_\mu} \frac{n_i}{n} + R_i. \tag{1}$$

n_i is the particle density of the (dust) species i under consideration, n is the total particle density of all species present in the mixture (determined by the H_2 and He density in our case), v_μ is the average particle velocity and D_{ig} is the binary diffusion coefficient for diffusion of the rare dust particles in the abundant carrier gas. R_i is the rate term for production or destruction of species i.

We assume that the turbulent flow responsible for the diffusion process is also responsible for the viscous evolution of the accretion disk[1]. Further we assume that the Schmidt number $Sc = \nu/D$ that relates the diffusion coefficient D to the coefficient of viscosity ν, in case of mixing due to turbulence is of the same order of magnitude as in the case of mixing by random thermal motions in a gas. In the latter case the Schmidt number is close to unity (e.g. Hirschfelder et al. 1964; Waldmann 1958) and, motivated by this, we approximate the diffusion coefficient by

$$D_{ig} = \frac{\nu}{Sc}, \tag{2}$$

where ν denotes the viscosity. This quantity is given by (42). For turbulent flows the ratio of the transport coefficient of some quantity to the transport coefficient of momentum, the inverse Prandtl number ($= Sc^{-1}$), can be determined by laboratory experiments. These numbers depend to some extent on the particular geometry of the flow system, but are generally found to be close to unity (cf. Launder 1976; McComb 1990), typically $Sc \approx 0.7$. In our calculations we use for the Schmidt number a value of

$$Sc = 1, \tag{3}$$

which probably slightly underestimates the efficiency of turbulent mixing. This guarantees that our result for mixing of dust species in the disc model does not overestimate the extent of mixing in a real disc.

The approximation (2) for the diffusion coefficient only holds for small particles which are strongly frictionally coupled to the carrier gas and are passively moved around with the turbulent flow. For conditions in protoplanetary discs at 1 AU this is satisfied for particles up to roughly 1 mm size (cf. Fig. 3 in Weidenschilling & Cuzzi 1993). The transport coefficient for diffusional mixing in the form (2) can be applied, thus, if dust coagulation at the onset of planetary formation has not yet proceeded so far that the first planetesimals start to form. This is exactly that phase of the disk evolution which we plan to consider. For bigger particles (2) cannot be applied; this case is considered, for instance, by Cuzzi et al. (1993) and Dubrulle et al. (1995).

We introduce cylindrical coordinates and assume all quantities in the disk to be independent of the azimuthal coordinate. Then Eq. (1) reads as follows

$$\frac{\partial n_i}{\partial t} + \frac{1}{r}\frac{\partial}{\partial r} r \left[n_i v_\mathrm{r} - D_{ig}\, n \frac{\partial}{\partial z}\frac{n_i}{n} \right] + \frac{\partial}{\partial z}\left[n_i v_z - D_{ig}\, n \frac{\partial}{\partial z}\frac{n_i}{n} \right] = R_i. \tag{4}$$

v_r is the radial drift velocity with which the disk material moves towards the star. Its magnitude is given by (47). Since the disk height decreases with decreasing distance to the protosun there is an associated slow vertical motion of the disk material towards the midplane with some

[1] Note that within the region $0.5 \lesssim r \lesssim 10$ AU of interest for mixing processes the disc material is only very weakly ionised (cf. Finocchi & Gail 1997; D'Alessio et al. 1998). Any magnetic instability which is often claimed to drive accretion cannot be active in regions where the electric conductivity of the disc material is very low and there is also not any necessity for assuming such a mechanism to be active in this region because the disc is convectively unstable.

velocity v_z. Its magnitude may be estimated by

$$v_z \approx \frac{\mathrm{d}h}{\mathrm{d}r}\frac{\mathrm{d}r}{\mathrm{d}t} = v_\mathrm{r}\frac{\mathrm{d}h}{\mathrm{d}r}$$
$$\approx 1\times 10^{-1}\,\frac{\mathrm{cm}}{\mathrm{s}}\; s^{\frac{1}{20}}\left(\frac{M}{M_\odot}\right)^{-\frac{3}{8}}\left(\dot{M}_{-7}\,\kappa\right)^{\frac{1}{8}}\mu^{-\frac{1}{2}}. \qquad (5)$$

The numerical value is derived for the semianalytical disc model in Duschl et al. (1996). s is the distance to the protostar in units of AU, κ is the mass extinction coefficient and μ the mean molecular weight. $\dot{M}_{-7}$ is the (stationary) mass accretion rate in units of $10^{-7}\,M_\odot\,\mathrm{yr}^{-1}$.

We estimate the relative order of magnitude of the terms which occur in the diffusion Eq. (4). First we estimate the order of magnitude of the radial diffusion term by $D_{ig}n_i/r$. The ratio of the radial diffusion term to the radial drift term is

$$\frac{D_{ig}n}{n_i v_\mathrm{r}}\frac{\partial}{\partial r}\frac{n_i}{n} \approx \frac{\nu}{r v_\mathrm{r}} = \frac{2}{3}. \qquad (6)$$

This relation is easily derived from the equations for a stationary accretion disc. Radial diffusion and radial transport by drift occur on a comparable timescale if the concentration of dust species varies on length scales of the order of the radial distance. For shorter length scales of the inhomogeneities in the material composition radial diffusional mixing is faster than transport by radial drift. Radial diffusive mixing, thus, is an important process for the determination of radial concentration profiles in a protoplanetary disc but does not dominate over radial transport by inwards drift of the disc material.

Next we estimate the order of magnitude of the vertical diffusion term by $D_{ig}n_i/h$. The ratio of the vertical diffusion term in Eq. (4) to the vertical drift term is

$$\frac{D_{ig}n}{n_i v_z}\frac{\partial}{\partial z}\frac{n_i}{n} \approx \frac{\nu}{h v_z} \approx 69\, s^{-\frac{1}{20}}\left(\frac{M}{M_\odot}\right)^{\frac{3}{8}}\left(\dot{M}_{-7}\,\kappa\right)^{-\frac{1}{8}}\mu^{\frac{1}{2}}. \qquad (7)$$

The numerical value is derived for the semianalytical disc model in Duschl et al. (1996). Since $M/M_\odot$, $\dot{M}_{-7}$, and μ usually are numbers of order unity and κ varies between $\approx$1 if dust extinction dominates and $\approx 10^{-4}$ if molecular opacity dominates, vertical diffusion always dominates over vertical drift. The vertical concentration profile is determined by vertical mixing by diffusion (and by the vertical distribution of sources or sinks, if such exist).

Finally we estimate the timescales for radial and vertical diffusion by

$$\tau_\mathrm{hor} = \frac{r^2}{\nu} = 2.7\times 10^4\ \mathrm{years}\ \cdot\ s^{\frac{7}{5}}\left(\dot{M}_{-7}\right)^{-1} \qquad (8)$$

and

$$\tau_\mathrm{vert} = \frac{h^2}{\nu} = 2.5\times 10^2\ \mathrm{years}\cdot s^{\frac{3}{2}}\left(\frac{M}{M_\odot}\right)^{\frac{3}{4}}\left(\dot{M}_{-7}\,\kappa\right)^{-\frac{1}{4}}\mu, \qquad (9)$$

respectively. We obtain

$$\frac{\tau_\mathrm{vert}}{\tau_\mathrm{hor}} = \frac{h^2}{r^2} \approx 10^{-2}. \qquad (10)$$

The numerical values, again, refer to the semianalytical disc model in Duschl et al. (1996). Radial mixing then occurs on a timescale comparable to the evolution time scale of the accretion disk while vertical mixing occurs nearly instantaneously as compared to the radial mixing time scale. We can assume, then, that the vertical abundance profile always has relaxed to a stationary state determined by the local physics. In the simple case that there are no local sources or sinks for a species the concentration of that species is constant in the vertical direction, but this is not necessarily the case for the radial direction if there are distant sources or sinks in other regions of the disc. If there exist vertically distributed sources or sinks the resulting vertical concentration profile depends on the ratio of the mixing time scale to the production and destruction time scales. We shall assume in our model calculation that the disc is well mixed in the vertical direction.

If we use particle concentrations $c_i = n_i/n$ instead of particle densities, assume cylindrical symmetry for the problem, and use the continuity equation for the total particle density

$$\frac{\partial n}{\partial t} + \frac{1}{r}\frac{\partial\, r n v_\mathrm{r}}{\partial r} = 0 \qquad (11)$$

the diffusion–transport–reaction equation takes the form

$$\frac{\partial c_i}{\partial t} + v_{\mathrm{r},\,i}\frac{\partial c_i}{\partial r} = \frac{1}{nr}\frac{\partial}{\partial r}\, r n D_i \frac{\partial c_i}{\partial r} + \frac{R_i}{n}. \qquad (12)$$

2.1. The rate term

We shall apply the diffusion–transport–reaction equation to an ensemble of dust grains which change their size by growth and/or destruction processes. We assume the grains to be spheres with radius a. For our further purposes we introduce a set of discrete grain radii a_i, $i = 1, \ldots, I$. a_1 is the radius of the smallest grain, a_I that of the biggest one. We define c_i to be the number of grains per H nucleus with radii in the interval between a_i and a_{i+1}. Since we have I discrete radii, we have $I-1$ such radius intervals and $I-1$ concentrations c_i. The numbers c_i ($i = 1, \ldots, I-1$) describe the size distribution of the grains.

For each group i of grains the radial and temporal variation of their concentration in the protoplanetary disc is described by an equation of the type (12). If we consider small grains which are efficiently coupled to the gas, the velocity $v_{\mathrm{r},\,i}$ is the radial drift velocity of the gas in the protoplanetary disk and D_i is the turbulence induced diffusion coefficient. In this case the drift velocities $v_{\mathrm{r},\,i}$ and the diffusion coefficients D_i are the same for particles of all groups i.

If we consider the problem of growth and destruction of grains the rate term R_i describes the change of the number of grains per H nucleus with radii between a_i and a_{i+1} per unit time due to the grain growth and destruction processes. For a single spherical grain the change of its

radius does not depend on its radius and is given by an equation of the type

$$\dot{a} = \frac{\mathrm{d}a}{\mathrm{d}t} = -V_0 \alpha n_\mathrm{g} v_\mathrm{th}.$$

The meaning of the different terms on the r.h.s. will be explained later. For the moment we assume that $\dot{a}$ is known. Within an interval of time Δt the radius of an individual grain changes by $\dot{a}\Delta t$. If $\dot{a} < 0$ then all grains which had at time t radii in the radius interval between a_{i+1} and $a_{i+1} + \dot{a}\Delta t$, are found at time $t + \Delta t$ inside the radius interval from a_i to a_{i+1} within Δt. The net gain of the radius interval $[a_i, a_{i+1}]$ within time Δt then is

$$c_{i+1} \frac{|\dot{a}|\Delta t}{a_{i+2} - a_{i+1}},$$

since c_{i+1} was the number of grains per H nucleus which had at time t radii in $[a_{i+1}, a_{i+2}]$ and the fraction $|\dot{a}|\Delta t/(a_{i+2} - a_{i+1})$ of them are lost to $[a_i, a_{i+1}]$. Analogously the loss of $[a_i, a_{i+1}]$ to $[a_{i-1}, a_i]$ is

$$c_i \frac{|\dot{a}|\Delta t}{a_{i+1} - a_i}.$$

Dividing by Δt and defining

$$\Delta a_i = a_{i+1} - a_i \tag{13}$$

yields the following form of the rate term in case of particle destruction

$$\frac{R_i}{n} = \left(\frac{c_{i+1}}{\Delta a_{i+1}} - \frac{c_i}{\Delta a_i} \right) \left| \frac{\mathrm{d}a}{\mathrm{d}t} \right| \quad \text{if} \quad \frac{\mathrm{d}a}{\mathrm{d}t} < 0. \tag{14}$$

For $i = I - 1$ the first term has to be omitted for obvious reasons. For $i = 1$ the second term is the rate of final loss of grains.

For the case of particle growth we find

$$\frac{R_i}{n} = \left(\frac{c_{i-1}}{\Delta a_{i-1}} - \frac{c_i}{\Delta a_i} \right) \frac{\mathrm{d}a}{\mathrm{d}t} \quad \text{if} \quad \frac{\mathrm{d}a}{\mathrm{d}t} > 0. \tag{15}$$

In this case the first term has to be omitted. If new grains with radii in $[a_1, a_2]$ are created, a production term for such grains has to be introduced instead of the term with index $i - 1$ in the equation with $i = 1$.

With this rate term, we have the following system of diffusion – transport – reaction equations for the concentration of grains of groups i

$$\frac{\partial c_i}{\partial t} + v_{\mathrm{r},i} \frac{\partial c_i}{\partial r} = \frac{1}{nr} \frac{\partial}{\partial r} rnD_i \frac{\partial c_i}{\partial r} + \begin{cases} \left(\frac{c_{i+1}}{\Delta a_{i+1}} - \frac{c_i}{\Delta a_i} \right) \left| \frac{\mathrm{d}a}{\mathrm{d}t} \right| & \text{if} \quad \frac{\mathrm{d}a}{\mathrm{d}t} < 0 \\ \left(\frac{c_{i-1}}{\Delta a_{i-1}} - \frac{c_i}{\Delta a_i} \right) \frac{\mathrm{d}a}{\mathrm{d}t} & \text{if} \quad \frac{\mathrm{d}a}{\mathrm{d}t} > 0 \end{cases}. \tag{16}$$

This couples each concentration c_i to c_{i-1} and c_{i+1}, except for the boundaries $i = 1$ and $i = I - 1$.

In applying this or Eq. (12) to an accretion disc in the one-zone approximation we have to take an average with respect to the z-direction. If the disc is well mixed in the vertical direction the c_i do not depend on z. The averaging procedure then has to be applied to the diffusion coefficient D and the rate term only. If D is calculated according to (2) with the viscosity calculated from the equations for the disc structure in the one-zone approximation then D is already the z-averaged diffusion coefficient since in the one-zone approximation ν is already averaged with respect to the z-direction.

3. Carbon combustion

Carbon dust is a very efficient absorber and accounts for a large fraction of the dust extinction which in turn determines the temperature structure in an accretion disc. A realistic modeling of the properties of a protoplanetary accretion disc requires the determination of the true spatial distribution of this dust component within the disc.

Since the material in a protoplanetary disc is oxygen rich ($\epsilon_\mathrm{C}/\epsilon_\mathrm{O} < 1$) solid carbon is only metastable in this environment. Its existence in the interstellar matter and in the cool parts of the disc solely rests on the fact that any oxidation reaction converting solid carbon into CO, the thermodynamically most stable carbon compound in most parts of the disk, is prevented by high activation energy barriers involved in any possible chemical reaction path for carbon oxidation. At sufficiently high temperatures, however, the solid carbon is converted into gaseous products by chemical surface reactions and subsequent reactions in the gas phase. If gas from warm disc regions where carbon dust is partially or completely destroyed is mixed by diffusion processes into cold disk regions, the carbon abundance in this region is reduced by dilution of the dusty gas with (carbon) dust free material. In the oxygen rich environments the gaseous products of carbon destruction cannot re-condense onto the surface of grains to restore the solid carbon content. One therefore expects a considerable modification of the abundance of carbon dust in cold parts of the disk by carbon destruction in the warm inner region of the disc and turbulent radial mixing of this material into the cold outer parts of the disc.

That carbon dust is not destroyed by vapourisation but by oxidation is shown in Finocchi et al. (1997).

3.1. Calculation of the carbon oxidation rate $\dot{a}$

The rate of carbon destruction depends on the nature of the carbon dust which is assumed to exist in the early phases of the evolution of the protoplanetary disc. We assume here that the carbon dust component is really carbon dust and not the carbonaceous material, the kerogen, found in CI meteorites, since the kerogen seems to be a product of chemical processes in the protoplanetary disc (e.g. Cronin et al. 1988), though a partial extrasolar origin cannot be excluded (e.g. Zinner 1988).

The oxidation process for solid carbon under conditions appropriate for the protoplanetary disc is discussed in detail in Duschl et al. (1996) and Finocchi et al. (1997)

and will not be repeated here. We only mention that the rate determining step for oxidation of solid carbon is the reaction of OH with an aromatically bound six-ring at the surface:

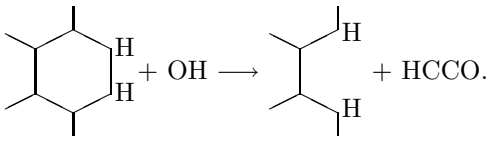

The change of radius a of a spherical carbon grain by this process is

$$\frac{\mathrm{d}a}{\mathrm{d}t} = V_{0,\mathrm{car}} \alpha_{\mathrm{ox}} n_{\mathrm{OH}} v_{\mathrm{th,OH}}. \tag{17}$$

$V_{0,\mathrm{car}}$ is the volume of a carbon atom in the solid, which is given by

$$V_{0,\mathrm{car}} = \frac{A m_{\mathrm{H}}}{\rho_{\mathrm{car}}}. \tag{18}$$

A is the atomic weight of carbon atoms and ρ_{car} the mass density of solid carbon. n_{OH} and $v_{\mathrm{th,OH}}$ are the density of OH radicals and their root mean square thermal velocity, respectively. α_{ox} is the probability that a collision of a OH molecule with the surface of solid carbon cracks carbon-carbon bonds and injects carbon into the gas phase. The coefficient α_{ox} of the oxidation reaction rate has been determined by laboratory experiments to be $\approx$0.2 (cf. Finocchi et al. 1997). Since each reaction removes two carbon atoms from the grain we choose $\alpha_{\mathrm{ox}} = 0.1$ in our calculation.

For calculating $\dot{a}$ one has to know the abundance of the OH radical in the disc in a zone where the oxidation reaction occurs, i.e., at a temperature of about 1000 K. Our previous calculations (Finocchi et al. 1997; Finocchi & Gail 1997) of the non-equilibrium chemistry in a protoplanetary disk have shown that the O–H – chemistry in this region essentially is in chemical equilibrium. Since mixing timescales in the vertical direction are of the order of centuries (cf. Eq. (9)) we also can assume chemical equilibrium with respect to the vertical distribution of OH molecules at the temperatures of interest. We therefore calculate the OH abundance by solving the appropriate equations for the equilibrium chemistry simultaneously with the equations for the disc structure.

In principle we have to use for n_{OH} the average with respect to the z-direction. The OH concentration well below the dissociation limit of H_2O depends strongly on the temperature which is not constant in the vertical direction. This means that we cannot calculate the z-average of n_{OH} without calculating the detailed vertical disc structure. Within the frame of the one-zone approximation we can only determine n_{OH} at the midplane of the disk. If we use this n_{OH} in (17) the oxidation rate for carbon is somewhat overestimated, but not seriously. Since T is highest in the midplane and the oxidation rate depends steeply on temperature, a carbon grain is oxidised during that part of its random walk induced by turbulence where it is close to the midplane in a region where the temperature is close to the midplane temperature. The z-averaging procedure in principle corresponds to multiplying the density of OH at the midplane by the ratio of the half-width of the temperature peak around the midplane to the disk height, which is smaller than unity but not a small quantity since most of the temperature decline from the midplane to the surface temperature T_{eff} occurs near the surface. Thus, within the frame of the accuracy which can be achieved with disc models in the one-zone approximation one can replace the z-averaged n_{OH} by its midplane value in (17).

3.2. Solution of the diffusion-transport-reaction equation

A modelling of carbon combustion within the frame of the one-zone approximation requires one to solve the set of diffusion-transport-reaction Eq. (16) for the discrete size distribution c_i of the carbon dust grains. Since carbon dust in an oxygen rich environment is only destroyed and cannot recondense, we have in this case always $\dot{a} < 0$. The system of equations then has the convenient property that the equation for some particular c_i is coupled only with the equation for c_{i+1}, but not with the equation for c_{i-1}. For the equation for the uppermost size interval $[a_{I-1}, a_I]$ there is no coupling term to a size interval for bigger grains, i.e., the equation for c_{I-1} can be solved directly without any knowledge of the concentration in another size interval. The solution algorithm for the system of Eq. (16) then is as follows: first one solves the equation for the concentration c_{I-1} of the biggest grains and then one successively solves the equations for $i = I-2, \ldots, i = 1$ using in each case the result for c_{i+1} in the equation for c_i.

In a stationary disc the system of diffusion equations reduces to a coupled system of second order ordinary differential equations. The solution of such a system requires the prescription of two boundary conditions for each equation. The natural boundary conditions for our present problem are as follows:

1) For modelling the protoplanetary accretion disc we chose an inner disk radius sufficiently small such that there exists no dust at this radius. Then one simply has

$$c_i = 0 \quad i = 1, \ldots, I-1 \tag{19}$$

at the inner boundary.

2) The outer radius is chosen at a large distance where the dust mixture is expected to resemble the unmodified dust from the parent molecular cloud. We assume that the size distribution in this case is given by the Mathis-Rumpl-Nordsieck (1977) size distribution

$$f(a) = \begin{cases} 0 & \text{for } a < a_l \\ K\, a^{-3.5} & \text{for } a_l \le a \le a_u \\ 0 & \text{for } a_u < a \end{cases} \tag{20}$$

with $a_l = 0.005\,\mu$m and $a_u = 0.25\,\mu$m. The constant K is fixed by the requirement that

$$\int_{a_l}^{a_u} \frac{4\pi}{3} a^3 f(a) \mathrm{d}a = V_0 f_{\mathrm{car},0}\, \epsilon_{\mathrm{C}}. \tag{21}$$

$\epsilon_{\rm C}$ is the total abundance of carbon nuclei with respect to H nuclei and $f_{\rm car,0}$ is the fraction of the carbon condensed into carbon grains in the parent molecular molecular cloud, for which we assume a value of 0.6 (Mathis et al. 1977). The initial values for c_i at the outer boundary then are

$$c_i = \int_{a_i}^{a_{i+1}} f(a)\,{\rm d}a. \tag{22}$$

From the solutions c_i of the diffusion – transport – reaction equations one calculates at any instant the fraction $f_{\rm car}$ of the total carbon condensed into grains from

$$f_{\rm car} = \frac{1}{V_0\epsilon_{\rm C}} \sum_{i=1}^{I-1} c_i\,\frac{4\pi}{3}a_i^3, \tag{23}$$

where Riemann sums are used for evaluating numerically the integral (or any other sum formula). This $f_{\rm car}$ is required to calculate the contribution of carbon grains to the opacity of the disc material.

4. Annealing

The silicate dust component from the parent molecular cloud enters the protoplanetary accretion disc with an amorphous lattice structure. In a region of the disc where the midplane temperature exceeds ≈800 K (Duschl et al. 1996; Gail 1998) activation of internal rearrangement processes in the lattice lead to the development of a crystalline lattice structure (annealing). Since amorphous and crystalline silicate have drastically different extinction properties (cf. Fig. 1), the process of annealing has strong implications for the structure of the protoplanetary disk. Especially, if turbulent mixing processes transport crystallised silicate dust from the warm inner disc into the outer disc regions, the dust opacity in that region is reduced. It is important, thus, to account for the annealing and mixing process if the structure of a protoplanetary disc is calculated.

4.1. Annealing of silicate dust

In Gail (1998) the process of transformation of the amorphous lattice structure of dust grains into a more organised microcrystalline structure at temperatures $\lesssim 1000\,{\rm K}$ was treated by a simple approximation. It was assumed that within the lattice of the initially amorphous dust grains from the parent molecular cloud, which show a high degree of disorder in the spatial arrangement of the basic SiO_4 tetrahedrons, there exist some tiny regions with a highly regular arrangement of the SiO_4 tetrahedrons. Such islands of small scale order always exist in a disordered solid, at least for pure statistical reasons. These regions then may serve as growth centres which grow into their disordered environment by internal rearrangement processes if such processes are activated at sufficiently high temperature[2]. The increase of the volume $V_{\rm cr}$ of the crystallised regions approximately is given by (Gail 1998)

$$\frac{{\rm d}V_{\rm cr}}{{\rm d}t} = 6V_0^{\frac{1}{3}}V_{\rm cr}^{\frac{2}{3}}\nu_{\rm vib}{\rm e}^{-E_{\rm a}/kT}. \tag{24}$$

Here V_0 is the volume of the crystallised silicate per SiO_4 tetrahedron, which is simply determined by the atomic weight A of the compound and the mass density $\rho_{\rm s}$ of the solid as in Eq. (18). $\nu_{\rm vib}$ is the characteristic frequency of the lattice vibrations and $E_{\rm a}$ is the activation energy for the internal rearrangement processes, which are responsible for annealing. Equation (24) is valid as long as the crystallised regions are isolated and grow independently of each other. In the late phases of the annealing process, when crystallised regions come into contact, Eq. (24) overestimates the growth of the crystallised region since the ratio of active growth surface to volume, which is assumed to be constant in (24), rapidly changes in this phase. Since Eq. (24) is already a strongly simplifying approximation we ignore this complication and use (24) also in the late phases of annealing.

The activation energy for annealing of silicate grains can be determined from the change of extinction properties of interstellar dust analogues by annealing. In Lenzuni et al. (1995) and Duschl et al. (1996) an activation energy of $E_{\rm a}/k = 41\,000\,{\rm K}$ was derived in this way from the annealing experiment of Nuth & Donn (1982), assuming a characteristic frequency of $\nu_{\rm vib} = 2\times10^{13}\,{\rm s}^{-1}$. This activation energy, however, probably refers to the formation of Si_2O_3. The new laboratory experiments on silicate annealing of Hallenbeck et al. (1998, 2000) yield approximately the same activation energy. Brucato et al. (1999) performed annealing experiments for pyroxene and obtained $E_{\rm a}/k = 47\,500\,{\rm K}$. Fabian et al. (2000) performed detailed new experiments on annealing of glassy forsterite, enstatite, and quartz and obtained activation energies for annealing of $E_{\rm a}/k = 39\,100 \pm 400$, $42\,040 \pm 150$ and $49\,190 \pm 150\,{\rm K}$ for these three materials, respectively. In our calculation we use the results of Fabian et al. (2000) for $E_{\rm a}$.

If we assume that initially we have a fraction of $\zeta_{\rm cr}$ of growth centres for crystallisation per silicon atom, then the number of such centres within a dust grain of volume V is

$$N_{\rm cr} = \zeta_{\rm cr}\frac{V}{V_0}, \tag{25}$$

since V/V_0 is the number of silicon atoms in the grain. The choice of $\zeta_{\rm cr}$ is described below. The average volume into which a growth centre can expand is $V/N_{\rm cr}$ and the actual volume $V_{\rm cr}$ of each crystallised region divided by the available volume $V/N_{\rm cr}$ is the fraction of the total volume

[2] A completely different point of view has been taken by Sogawa & Kozasa (1999) for the analogous problem of formation of crystalline dust in circumstellar dust shells. Since calculations of nucleation rates for crystallisation centres based on classical nucleation theory do not yield reliable results, we follow the simpler approach used in this paper.

which is already crystallised. Thus we define the degree of crystallisation of the grain material by

$$x_{\rm cr} = \min\left(\frac{\zeta_{\rm cr} V_{\rm cr}}{V_0}, 1\right). \tag{26}$$

From this definition we find

$$\frac{{\rm d}x_{\rm cr}}{{\rm d}t} = \begin{cases} 6 x_{\rm cr}^{\frac{2}{3}} \zeta_{\rm cr}^{\frac{1}{3}} \nu_{\rm vib} {\rm e}^{-E_{\rm a}/kT} & \text{for } x_{\rm cr} < 1 \\ 0 & \text{else} \end{cases}. \tag{27}$$

It is then advantageous not to consider $x_{\rm cr}$ itself but instead of this the variable

$$\xi = x_{\rm cr}^{\frac{1}{3}} \tag{28}$$

since for this we have

$$\frac{{\rm d}\xi}{{\rm d}t} = \begin{cases} 2 \zeta_{\rm cr}^{\frac{1}{3}} \nu_{\rm vib} {\rm e}^{-E_{\rm a}/kT} & \text{for } \xi < 1 \\ 0 & \text{else} \end{cases} \tag{29}$$

where now the r.h.s. does not depend on the variable ξ. For mathematical reasons, in the following we work only with the variable ξ, but note that the third power of ξ and not ξ itself is the true degree of crystallisation.

If we start with completely amorphous grains, i.e. $\xi = 0$, and integrate (29) we get

$$\xi(t) = \min\left[2 \zeta_{\rm cr}^{\frac{1}{3}} \nu_{\rm vib} \int_{-\infty}^{t} {\rm d}u \, {\rm e}^{-E_{\rm a}/kT(u)}, \; 1\right]. \tag{30}$$

The degree of crystallisation ξ^3 of a grain depends on its past thermal evolution. Since the exponential increases very steeply with increasing T the integral is determined by the highest temperature(s) the particle has experienced so far. If we expand in the exponential $1/T$ around the instant t_i of a temperature maximum correct up to the second order in $(t - t_i)$ (the first derivative vanishes at the maximum) and integrate the resulting Gaussian, then we obtain

$$\xi(t) = 2 \zeta_{\rm cr}^{\frac{1}{3}} \nu_{\rm vib} \sum_i {\rm e}^{-T_0/T_i} \sqrt{\frac{\pi T_i^3}{T_0} \left|\frac{{\rm d}^2 T}{{\rm d}t^2}\right|_{t_i}^{-1}}, \tag{31}$$

where the sum runs over the highest temperature maxima experienced by a grain during its past history. Obviously only the term(s) corresponding to the highest temperature the grain ever has experienced will really contribute to the sum.

Dust grains in a protoplanetary accretion disk are moved around by turbulent convective motions of the carrier gas. They are permanently carried from the warm midplane of the disk to the cold disk surface and back, and they are carried back and forth between the hot inner and cold outer parts of the disk. Then $\xi(t)$ as a function of time has a step-like character: during short periods where the grain visits hot parts of the disk the degree of crystallisation ξ^3 rapidly increases. Such events are interrupted by periods during which the grain stays in cold parts of the disk and ξ practically does not change.

4.2. Calculation of the annealing and mixing of silicate dust

As a result of turbulent mixing at each instant and each point of the disk one encounters grains with completely different temperature histories due to their random walk in the disk induced by the turbulent motions. The maximum temperatures which the grains have experienced during their past are very different and, thus, their degree of crystallisation may take any value between 0 and 1. The degree of crystallisation of such a mixture of grains is most conveniently described by a probability density. At this place we note that within the frame of our simple model for the annealing process the rate of change of the crystallinity of a grain (29) does not depend on the grain size. Grains with different radii but the same temperature history have the same degree of crystallinity. This may not be completely realistic, but allows for the simple model of annealing used in this paper to define a probability density in a unified way for all grains consisting of the same type of material, irrespective of their size. Denote this probability density with respect to ξ at position r and instant t by $c(t, r, \xi)$. This quantity has the following meaning: $c(t, r, \xi)\Delta\xi$ is the probability that grains at position r and instant t have a degree of crystallisation in the interval $[\xi^3, (\xi + \Delta\xi)^3]$. It is our aim to calculate this quantity for the silicate dust in the protoplanetary disk[3].

For calculating the probability density c, we proceed in a manner analogous to the case of carbon combustion. We replace the continuous ξ-scale by a discrete set of gridpoints ξ_i $(i = 1, \ldots, I)$ where $x_1 = 0$ corresponds to completely amorphous grains and $x_I = 1$ to completely crystalline grains. We denote by c_i the fraction of grains for which ξ is between ξ_i and ξ_{i+1}. We have $I - 1$ such groups of grains and the set of numbers c_i is a discrete version of the probability distribution for the degree of crystallisation of dust grains. Note that according to the definition of c_i we have

$$\sum_i c_i = 1. \tag{32}$$

The temporal and spatial distribution of a mixture of grains of different degrees of crystallinity ranging from completely amorphous to completely crystallised grains is described by a set of equations of the type (12). The rate term on the r.h.s. of (12) in the present case is obtained in complete analogy to the derivations in Sect. 2.1 as

$$\frac{R_i}{n} = \left(\frac{c_{i-1}}{\Delta\xi_{i-1}} - \frac{c_i}{\Delta\xi_i}\right) \frac{{\rm d}\xi}{{\rm d}t} \tag{33}$$

[3] The definition of this probability has some problems for the following reason: if the dust material progressively crystallises due to annealing the degree of crystallisation for all grains tends to $\xi^3 = 1$. Ultimately all grains are completely crystallised. This means that the probability density in ξ finally tends to a δ distribution, defined on $[0, 1]$ and centred on $\xi = 1$. This leads to some mathematical complications. For numerical calculations this property is uncritical, since always intervals in ξ of finite widths are considered.

where $\dot{\xi}$ is given by (29) and $\Delta\xi_i$ is defined by

$$\Delta\xi_i = \xi_{i+1} - \xi_i. \tag{34}$$

In applying this to a one-zone model for a protoplanetary accretion disc we have to take an average with respect to the z-direction. Due to the non-constancy of T with z and the exponential dependence of $\dot{\xi}$ on T the rate term is strongly peaked to the midplane. Without a detailed knowledge of the vertical disc structure we cannot determine the z-average of $\exp(-E_\mathrm{a}/kT)$; we can only determine its value at the midplane. On the other hand, our model for the annealing process depends on the quantity ζ_cr which is only poorly determined. All uncertainties with respect to the averaging procedure for the exponential then can be absorbed in the definition of ζ_cr, which is specified below, and we simply use the midplane temperature for calculating $\dot{\xi}$.

The set of equations for c_i has the convenient property that the equation for c_i is coupled with the equation for c_{i-1}, but not with that for c_{i+1}. In the equation for c_1 there is no coupling term to c_{i-1}. Then we can solve the system by first solving the equation for c_1 and then successively for all equations with $i > 1$.

Again we consider a stationary protoplanetary disk in which case the set of diffusion – transport – annealing equations simplifies to a set of ordinary second order differential equations. The boundary conditions required to uniquely specify the solution are as follows:

1) The inner boundary of the disc is chosen at such a small radius that all mineral grains are crystallised or even vaporized in the innermost part of the disc model. Then all grains are found within the group c_{I-1} and we have

$$c_i = \begin{cases} 0 & \text{for } i = 1, \ldots, I-2 \\ \\ 1 & \text{for } i = I-1 \end{cases} \tag{35}$$

at the inner boundary.

2) The outer boundary of the disc is chosen at such a big radius that all mineral grains are amorphous in the outer parts of the disc. This corresponds to the assumption that the outermost parts of the disc contain only material collected from the parent molecular cloud. Then all grains are found within the group c_1 and we have

$$c_i = \begin{cases} 1 & \text{for } i = 1 \\ \\ 0 & \text{for } i = 2, \ldots, i = I-1 \end{cases} \tag{36}$$

at the outer boundary.

From the solutions c_i of the diffusion – transport – annealing equations one finds the average degree of crystallisation as

$$f_\mathrm{cr} = \sum_{i=1}^{I-1} \xi_i^3 c_i. \tag{37}$$

This quantity is required for calculating the contribution of silicate dust to the opacity of the disc material.

The rate (29) depends on the unknown parameter ζ_cr which is arbitrarily set to $\zeta_\mathrm{cr} = 10^{-5}$. Due to the very steep dependence of $\dot{\xi}$ on T the outcome for the temperature where annealing takes place depends only very weakly on the precise choice of ζ_cr. It can be varied by several orders of magnitude without changing the annealing temperature by more than $\pm 20\,\mathrm{K}$ (cf. Eq. (70) of Gail 1998[4]).

The model adopted for treating the annealing process loses its validity for the smallest grains with sizes of a few nm and less. It requires that there always exist at least a few growth centres within a grain. This is not guaranteed for the smallest grains which may even contain no growth centres. At this size level a probabilistic treatment of the annealing problem would be required which, however, is out of the scope of this paper. In any case, the population of extremely small grains contains a negligible fraction of the total dust mass and, thus, has no significant influence on the disc structure.

5. Model calculation

We construct protoplanetary disc models in the one-zone approximation for the inner part of a protoplanetary accretion disc, where the disc may be considered to be approximately stationary (cf. Ruden & Lin 1986). The model considers (i) the radial mixing of amorphous and crystalline silicate grains and (ii) the oxidation of carbon grains and the resulting dilution of carbon dust by radial mixing of carbon dust free matter from the inner region of the disk into the outer zones of the disc.

5.1. Equations for the radial disc structure

The basic set of equations describing the radial structure of a stationary, thin, Keplerian α-disc in the one-zone approximation is (e.g. Lin & Papaloizou 1985; Pringle 1981):

1) The Keplerian angular velocity of disc rotation:

$$\Omega = \sqrt{\frac{GM_*}{r^3}}. \tag{38}$$

M_* is the mass of the central protostar. The stellar mass is assumed to be constant with time.

2) The effective temperature of the disc surface:

$$T_\mathrm{eff}^4 = \frac{3GM_*\dot{M}}{\sigma_\mathrm{SB}\,8\pi r^3}\left(1 - \sqrt{\frac{R_*}{r}}\right). \tag{39}$$

σ_SB is the Stefan-Boltzmann constant. A contribution to the heating of the disc (i) by the energy liberated by the accretion shock, and (ii) by the illumination of the disc by the protostar, is not considered.

3) The isothermal sound velocity:

$$c_0 = \frac{kT_\mathrm{c}}{\mu m_\mathrm{H}}. \tag{40}$$

[4] Note that a different notation for the variables is used in that paper.

T_c is the temperature at the midplane of the disc, μ the mean molecular weight.
4) The vertical equivalent height of the disc:

$$h = \sqrt{\frac{\pi}{2}}\,\frac{c_0}{\Omega}. \tag{41}$$

5) The coefficient of viscosity in the α-approximation of Shakura & Sunyayev (1973):

$$\nu = \alpha h c_0. \tag{42}$$

h is the characteristic scale height of the disc, c_0 the isothermal velocity of sound in the midplane of the disc, and α the viscosity parameter introduced by Shakura & Sunyayev (1973). This ν determines according to (2) the diffusion coefficient D in the diffusion–transport–reaction Eq. (16).
6) The equation of angular momentum conservation:

$$\nu\Sigma = \frac{\dot{M}}{3\pi}\left(1 - \sqrt{\frac{R_*}{r}}\right). \tag{43}$$

ν is the viscosity, R_* the radius of the protostar. This equation determines the surface density Σ of the disc.
7) The mass density at the midplane:

$$\rho_c = \frac{1}{2}\frac{\Sigma}{h}. \tag{44}$$

8) The vertical optical depth at the midplane:

$$\tau_c = \frac{1}{2}\Sigma\,\kappa_R(\rho_c, T_c). \tag{45}$$

$\kappa_R(\rho_c, T_c)$ is the Rosseland-mean of the mass extinction coefficient of the disk material at the midplane.
9) The temperature at the midplane:

$${T_c}^4 = T_{\rm mol}^4 + \tfrac{1}{2}T_{\rm eff}^4\left[1 + \tfrac{3}{2}\tau_c\right]. \tag{46}$$

$T_{\rm mol}$ is the temperature of the ambient molecular cloud.
10) The equation of mass conservation:

$$\dot{M} = 2\pi r \Sigma v_r. \tag{47}$$

$\dot{M}$ is the accretion rate (constant in a stationary disc), Σ the surface density and v_r the (slow) inwards directed accretion velocity of the disc material. This equation determines v_r in the diffusion–transport–reaction Eq. (16).
11) The pressure at the midplane (equation of state):

$$P_c = c_0^2\rho_c. \tag{48}$$

12) This set of equations is completed by the two constitutive equations

$$\mu = \mu(\rho, T) \tag{49}$$

$$\kappa_R = \kappa_R(\rho, T), \tag{50}$$

which have to be determined from the chemical composition of the disc material and from the extinction properties of the dust and the gas phase species.

The equations depend on five free parameters: the stellar mass M_* and radius R_*, the accretion rate $\dot{M}$, the temperature of the molecular cloud $T_{\rm mol}$, and the constant α for the viscosity. Our particular choice for these parameters is described in Sect. 6.1.

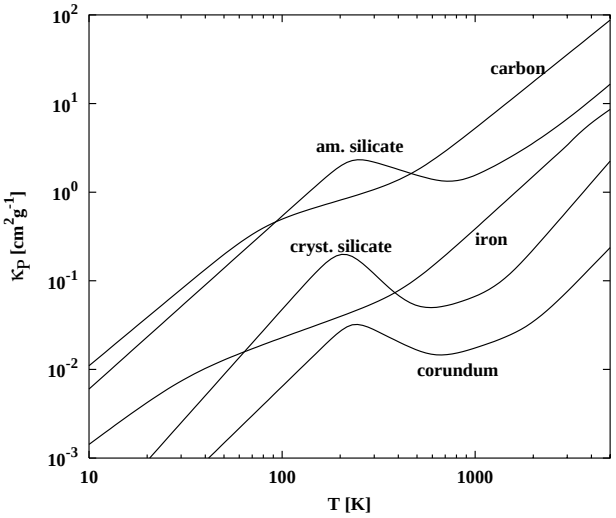

Fig. 1. Variation of the Rosseland mean extinction coefficient of the abundant dust species with the temperature of the local radiation field. Note the large difference between the opacities of amorphous and crystalline silicates. The silicate extinction is for olivine.

The set of Eqs. (40) ... (50) is solved by assuming a temperature T_c in Eq. (40) and solving Eqs. (40) ... (46) for a new value of T_c. Then T_c is iterated for self-consistency. A model is calculated for a set of radial grid points r_j between an inner boundary at $5\,R_*$ and some outer boundary for which we choose $r = 100\,\mathrm{AU}$. The inner boundary is chosen at such a radius that the temperature at this point (i) is sufficiently high for all possible dust materials to be vapourised at this temperature, and (ii) that at the same time it is sufficiently low for the extinction not to be dominated by H^- absorption in order to avoid the thermal-viscous instability associated with the steep rise of extinction with temperature in the region of dominating H^- extinction. The outer radius is chosen at a rather large distance for the reason that the boundary conditions for the radial diffusion-transport equations should be prescribed as far as possible in the outer region of the disc. This choice of the position of the outer boundary is larger than the outermost radius up to where the assumption of a stationary disc structure is reasonable (cf. the time dependent models calculated by Ruden & Lin 1986), i.e. the model calculated cannot be taken seriously in the region $r \gtrsim 20\,\mathrm{AU}$.

5.2. Opacity of the disc material

The disk opacity is determined by the various dust components present in the disk material and by the gas component in the dust free region. For determining the temperature in the disc from (45) and (46) the Rosseland mean opacity κ_R defined by

$$\kappa_R^{-1} = \int_0^\infty \kappa_\nu^{-1}\,\frac{\partial B_\nu(T)}{\partial T}\,\mathrm{d}\nu \Big/ \int_0^\infty \frac{\partial B_\nu(T)}{\partial T}\,\mathrm{d}\nu \tag{51}$$

is required. κ_ν is the frequency dependent extinction coefficient and B_ν the Kirchhoff-Planck function. The flux averaged mass extinction coefficient $\kappa_{\rm R}$ of the mixture of gas and dust is assumed to be given by

$$\kappa_{\rm R} = \kappa_{\rm gas} + \sum_i f_i \kappa_{i,\rm dust}. \tag{52}$$

Here we have assumed that the individual contributions $\kappa_{i,\ \rm dust}$ of all the species simply add up, an assumption which is generally not valid for the Rosseland mean of the extinction coefficient, except in the case of grey extinction. Since the dust extinction in the wavelength region ($\lambda \gtrsim 1.5\,\mu$m) where most of the energy is emitted and transported within the disk varies only slowly with wavelength, the dust absorbs nearly grey and the calculation of $\kappa_{\rm R}$ by simply adding up the separate contributions of the different dust species is sufficiently accurate.

In the model calculation we consider the following dust species: silicate grains with amorphous and crystalline lattice structure, iron grains, carbon grains and, as a representative of the class of the very stable Al and Ca compounds, corundum. At low temperatures a coating by water ice is considered. In a real accretion disc there exist additional dust components, which are not considered in the present model since our sample of dust species already accounts for the most important opacity sources.

The mass extinction coefficient $\kappa_{i,\ \rm dust}$ for the different dust components is calculated by assuming that the key element required for its formation (this usually is the least abundant of the elements required for the formation of the solid species) is completely condensed into this dust species. Since in the warm part of the disk condensation is not complete, the extinction coefficient $\kappa_{i,\ \rm dust}$ has to be multiplied by the fraction f_i of the key element, which really is condensed into dust species i. This f_i is determined in our model

- for the carbon dust component from the calculation of carbon destruction by oxidation;
- for the other dust species by calculating the degree of condensation of the species for a chemical equilibrium state.

For the silicate dust we consider that part of the grain population has an amorphous lattice structure and the other part a crystalline structure. The opacity of the mixture of amorphous and crystalline silicate grains is approximated by

$$\kappa_{\rm R,\ silicate} = f_{\rm cr}\kappa_{\rm R,\ crystalline\ sil.} + (1-f_{\rm cr})\,\kappa_{\rm R,\ amorphous\ sil.}. \tag{53}$$

$f_{\rm cr}$ is the fraction of the silicate dust which is crystalline. This is calculated according to (37). For $\kappa_{\rm R,\ crystalline\ sil.}$ we use data for olivine as a representative of this class of silicate grains. We do not discriminate between olivine and orthopyroxene.

The Rosseland mean $\kappa_{\rm R}$ for the individual dust components are calculated from optical constants and Mie theory. A Mathis-Rumpl-Nordsieck size distribution has been assumed. Details are described in Gail (1998) and Gail & Sedlmayr (1999). Figure 1 shows $\kappa_{\rm R}$ for the dust species included in the model calculation.

For ice coated grains and the gas extinction we use the approximation given in Bell & Lin (1994).

5.3. The equation of state

The equation of state is calculated in a simple approximation which concentrates on (i) the few elements which are important for determining the mean molecular weight $\mu(\rho, T)$, (ii) the gas phase species important for carbon combustion, and (iii) the degree of condensation of the refractory elements into the minerals which are considered in the model calculation.

5.3.1. The gas phase

The composition of the gas phase is solved for a state with given temperature T and density ρ as follows: first we take advantage of the fact that hydrogen and He are much more abundant than any of the other elements and that at the rather low pressures and temperatures of interest only H, H_2, and He are present. Any other compounds of hydrogen with less abundant elements and H ionisation can be neglected for calculating the dissociation equilibrium in the protoplanetary disc. The fictitious pressure $P_{\rm H}$ of H nuclei if all H nuclei would be present as the free neutral atom is determined by the mass density ρ according to

$$P_{\rm H} = \frac{\rho}{m_{\rm H}\left(1+\sum A_i\epsilon_i\right)}. \tag{54}$$

A_i are the atomic weights and ϵ_i the abundances of the elements.

The dissociation state of hydrogen in the warm parts of the protoplanetary disc corresponds to a chemical equilibrium state. From the law of mass action follows the equation

$$P_{\rm H} = p_{\rm H} + 2p_{\rm H}^2\,K_{\rm p}({\rm H_2}) \tag{55}$$

for the partial pressure $p_{\rm H}$ of free H atoms. $K_{\rm p}$ is the constant of the law of mass action for the H_2 molecule. In the cold parts of the disc which are penetrated by cosmic rays and where the density is low the chemical state of the disc material does not correspond to chemical equilibrium (Finocchi & Gail 1997), but the chemistry in this part is of no interest for calculating the rate of carbon oxidation.

From the solution of (55) the mean molecular weight μ follows as

$$\mu = \frac{2(1+4\epsilon_{\rm He})\,P_{\rm H}}{(1+2\epsilon_{\rm He})\,P_{\rm H} + p_{\rm H}}. \tag{56}$$

For oxygen one has to consider the following oxygen bearing gas phase species: CO, which binds all the carbon present in the gas phase, SiO which binds all the Si present in the gas phase, and OH, H_2O which bind the remaining fraction of the oxygen in the gas phase. Additionally,

a considerable fraction of the O is bound in solids. For simplicity we assume that only forsterite Mg_2SiO_4 and corundum Al_2O_3 are of interest. Then in chemical equilibrium the partial pressure p_O of free oxygen atoms is given by

$$\left(\epsilon_O - (1-f_{car})\epsilon_C - (1+3f_{for})\epsilon_{Si} - \frac{3}{2}f_{cor}\epsilon_{Al}\right) P_H = p_O\left(1 + p_H K_p(OH) + p_H^2 K_p(H_2O)\right). \quad (57)$$

f_{for}, f_{cor}, and f_{car} are the fraction of the Si condensed in forsterite, the fraction of the Al condensed in corundum and the fraction of the C bound in carbon grains, respectively. Other O bearing gas phase species have low abundance and can be neglected.

At the temperatures of interest the carbon in the gas phase is present as CO. We assume that any formation of CH_4, which would be the dominating C bearing gas phase species in some fraction of the cold part of protoplanetary disc, is suppressed for kinetic reasons (e.g. Fegley & Prinn 1989). Other C bearing gas phase species have low abundances and can be neglected.

5.3.2. The solids

For the solids we need in the present model calculation only to know how they vapourise at their upper stability limit since this determines the temperature structure in the warm part of the disk. This allows us to restrict our considerations to only three dust components: Corundum as a representative of the group of the most stable Ca-Al-dust components, to solid iron, and to forsterite which is the most thermodynamically stable of the silicate compounds. Since annealing of the amorphous dust components occurs at a temperature well below that of vaporisation of dust, the grains are crystalline when they vaporise. Further, in Duschl et al. (1996) it is shown that vapourisation occurs under conditions of quasi-stationarity. This allows to calculate the degree of condensation of the solids close to their stability limit from equilibrium thermodynamics. The degree of condensation of the dust species then is calculated as follows:

At temperatures $T > 1000\,\mathrm{K}$ where Mg is not completely bound in solids no abundant Mg bearing molecular species exists. Then we have for the partial pressure p_{Mg} of free Mg atoms in the gas phase

$$(\epsilon_{Mg} - 2f_{for}\epsilon_{Si})\, P_H = p_{Mg}. \quad (58)$$

The Solar System abundance of Mg is too low to allow for the condensation of all of the Si into Mg_2SiO_4 (forsterite) and for this reason large amounts of $MgSiO_3$ (enstatite) are formed in chemical equilibrium. For simplicity we neglect the formation of enstatite and, instead, artificially enlarge the Mg abundance to twice the Si abundance.

For silicon we assume that the only abundant gas phase species is SiO. We neglect the possibility that some fraction of the gas phase Si is bound in SiS, since this is unimportant for our present purposes. The partial pressure p_{Si} of free Si atoms in the gas phase in chemical equilibrium is given in this approximation by

$$(1-f_{for})\,\epsilon_{Si} P_H = p_{Si} p_O K_p(SiO). \quad (59)$$

If solid forsterite exists in chemical equilibrium with the gas phase, then the quantity (its activity)

$$a_{for} = p_{Si} p_{Mg}^2 p_O^4\, \mathrm{e}^{-\Delta G(for)/RT} \quad (60)$$

has to satisfy $a_{for} = 1$. ΔG(for) is the free enthalpy of formation of forsterite from the free atoms. Then, for calculating f_{for} we first put $f_{for} = 0$ in (59) and calculate p_{Si}. With this partial pressure of p_{Si} and the partial pressures p_{Mg} and p_O obtained from (58) and (57) we check whether $a_{for} < 1$. If this is true, no condensed forsterite exists and $f_{for} = 0$ is the correct solution. In the opposite case we re-calculate p_{Si} from (60) by letting $a_{for} = 1$ and then calculate $f_{for} > 0$ from (59).

For iron, as for Mg, no abundant molecular species exist in the gas phase. Thus we have for the partial pressure p_{Fe} of free Fe atoms in the gas phase

$$(1-f_{iro})\,\epsilon_{Fe} P_H = p_{Fe}. \quad (61)$$

If solid iron exists in chemical equilibrium with the gas phase, then

$$a_{iro} = p_{Fe}\, \mathrm{e}^{-\Delta G(iro)/RT} \quad (62)$$

has to satisfy $a_{iro} = 1$. ΔG(iro) is the free enthalpy of formation of solid iron from free atoms. For calculating f_{iro} we proceed as above: let $f_{iro} = 0$ in (61) and check with the resulting p_{Fe} whether $a_{iro} < 1$. If this is not true, then we determine p_{Fe} from (62) by letting $a_{iro} = 1$ and then calculate f_{iro} from (61).

For aluminium, besides free Al atoms Al_2O and AlOH are the most abundant gas phase species. For the partial pressure p_{Al} of free Al atoms we have the equation

$$(1-f_{cor})\,\epsilon_{Al} P_H = 2p_{Al}^2 p_O K_p(Al_2O) + p_{Al}\left(1 + p_H p_O K_p(AlOH)\right). \quad (63)$$

For solid corundum we have the equation

$$a_{cor} = p_{Al}^2 p_O^3\, \mathrm{e}^{-\Delta G(cor)/RT}. \quad (64)$$

Then p_{Al} and f_{cor} are calculated analogously as before, the only difference being that Eq. (63) now is a quadratic equation for p_{Al}.

The degree of condensation of f_{car} is calculated as described in Sect. 3.2. In the calculation of the equation of state f_{car} in (57) is assumed to be a given quantity. Thermodynamic data for calculating ΔG and K_p for the solids and molecules are taken from Sharp & Huebner (1990).

The complete set of Eqs. (57) ... (64) is solved in that sequence by first assuming $f_{for} = f_{cor} = 0$ in (57) and then iterating a few times using f_{for} and f_{cor} from the last iteration step in (57) until the accuracy of the solution is better than 10^{-8}.

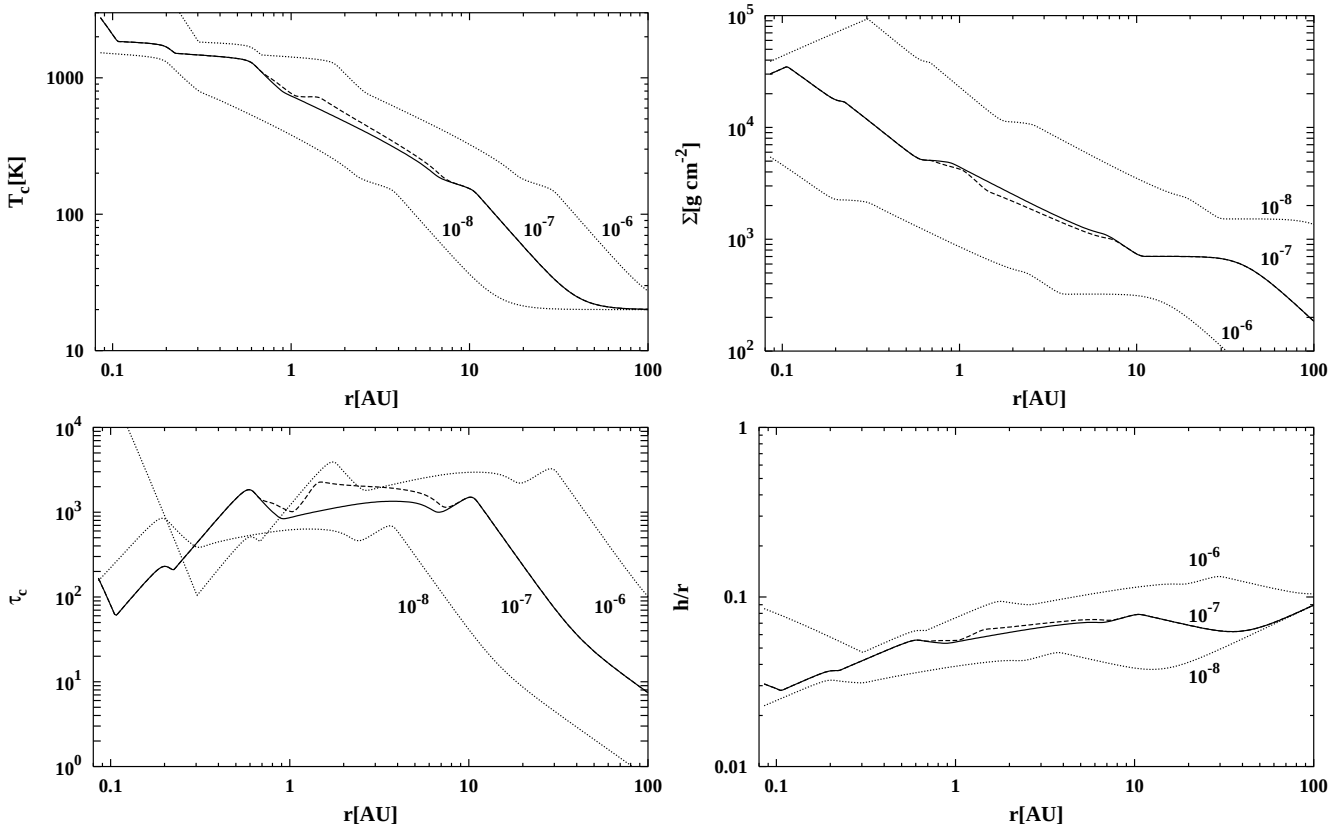

Fig. 2. Model of the radial disc structure with radial mixing by diffusion (full lines) and without mixing (dotted lines) for a mass accretion rate of $\dot{M} = 10^{-7}\,M_\odot\,\mathrm{yr}^{-1}$. *Top left:* temperature T_c at the midplane of the disk. *Top right:* surface density Σ of the disc. *Bottom left:* vertical optical depth τ_c at the midplane. *Bottom right:* vertical height h of the disk in units of the radius r (aspect ratio). Models for mass accretion rates of $\dot{M} = 10^{-6},\ 10^{-8}\,M_\odot\,\mathrm{yr}^{-1}$ with radial mixing are shown by dotted lines.

5.4. The diffusion − transport − reaction − equations

The radial diffusion and advection of the components of an inhomogeneous mixture of dust materials is described by Eq. (16). Here we consider two processes: (i) the problem of annealing the amorphous structure of pristine dust from the parent molecular cloud in the warm inner zone of the protoplanetary disk and mixing the crystallised grains outwards by diffusion and (ii) the combustion of carbon grains in the warm disc region and dilution of the dusty gas in the outer region with oxidised material from the inner zone by turbulent mixing. Equation (16) is solved numerically for the case of a stationary disc. For this purpose it is replaced by the difference equation

$$\frac{(rnD)_{j+\frac{1}{2}}\,(c_{i,j+1}-c_{i,j})}{n_j r_j\,h_{r,j}h_{m,j}} - \frac{(rnD)_{j-\frac{1}{2}}\,(c_{i,j}-c_{i,j-1})}{n_j r_j\,h_{l,j}h_{m,j}} - v_{r,j}\frac{c_{i,j+1}-c_{i,j}}{h_{r,j}} + \frac{R_{i,j}}{n_j} = 0 \quad (65)$$

for the discrete values of the concentrations $c_{i,j}$ at the radial grid points r_j. Here

$$h_{l,j} = r_j - r_{j-1} \quad (66)$$

$$h_{m,j} = \frac{1}{2}\,(r_{j+1} - r_{j-1}) \quad (67)$$

$$h_{r,j} = r_{j+1} - r_j. \quad (68)$$

Since in the stationary disc the drift velocity is directed inwards, we use for the advection term an upstream discretisation scheme. The rate term $R_{i,j}$ is given by (33) in the case of annealing and by (14) with $\dot{a}$ given by (17) in case of carbon combustion. n is the density of the H nuclei, given by P_H/kT (see Eq. (54)).

The set of equations for the $c_{i,j}$ for each $i = 1, \ldots, I-1$ forms a tridiagonal set of equations with respect to the index j for all j except for the first and last one which correspond to the boundaries. The $c_{i,j}$ at the boundaries are given as described in Sects. 3.2 and 4.2. These equations can easily be solved by standard methods.

The transport equations at present do not consider diffusional transport of molecular compounds of the refractory elements from the zone of vaporisation of minerals into cooler disc regions and their re-condensation, though this effect may be non-negligible (cf. the discussion in Mofill et al. 1985).

5.5. Calculation of the model structure

The complete set of equations for the disc structure including the radial transport processes, silicate annealing and carbon combustion is solved by a fixed-point iteration.

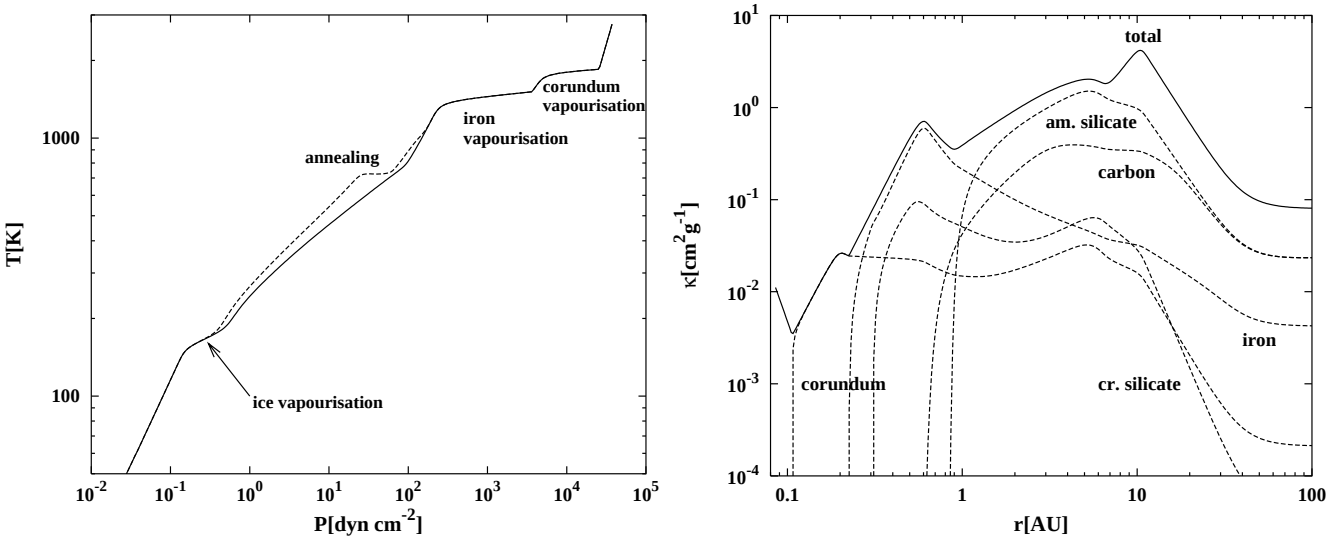

Fig. 3. *Left part:* pressure-temperature variation in the midplane of the disk. Indicated are the processes responsible for significant changes in the opacity. Full line: radial mixing included, dashed line: radial mixing omitted. *Right part:* radial variation of the total opacity (full line) in the midplane of the disk and contributions of the individual opacity sources (dashed lines) to the total opacity. Model for a mass accretion rate of $\dot{M} = 10^{-7}\,M_\odot\,\mathrm{yr}^{-1}$.

Table 1. Parameters used for the calculation of the disc model.

accretion rate	$\dot{M}$	$10^{-6}, 10^{-7}, 10^{-8}$	$M_\odot$ yr^{-1}
stellar mass	M_*	1	$M_\odot$
effective temperature	$T_{\rm eff}$	4500	K
stellar luminosity	L_*	5	$L_\odot$
viscosity parameter	α	3×10^{-3}	
molecular cloud temp.	$T_{\rm mol}$	20	K
inner disc radius	$r_{\rm in}$	5	R_*
outer disc radius	$r_{\rm out}$	100	AU

The equations for the disc structure and equation of state are solved at every radial grid point first by assuming the silicate dust grains to be amorphous and by assuming a constant fraction of the carbon to be bound in carbon grains. Then the equations for carbon combustion and radial transport and the equations for annealing and radial transport of silicate grains are solved. The resulting radial run of the fraction $f_{\rm car}$ of the carbon bound in carbon grains and the fraction $f_{\rm cry}$ of silicate grains with crystalline lattice structure then is used to calculate a new model for the radial disc structure. This procedure is repeated until the relative change of the variables between two iteration steps is less than 10^{-6}.

6. Results

6.1. Radial model structure

Models are calculated for a protostellar accretion disc around a single star with the set of parameters shown in Table 1. The stellar parameters correspond to a star of one solar mass in a stage of evolution where the star is already visible, i.e. the process of mass infall and star formation is nearly finished and the remaining disc gradually disappears by accretion onto the star (c.f. Stahler & Walter 1993). The viscosity parameter α is chosen such that it results in a timescale for disc disappearance in time dependent one-zone model calculations which is of the order of the observed timescale of roughly 10^7 years (Ruden & Pollack 1991). Slightly higher values for α are favoured by others (e.g. Lin & Papaloizou 1996; Stepinski 1998).

The calculation assumes a mass accretion rate of $\dot{M} = 10^{-7}\,M_\odot\,\mathrm{yr}^{-1}$. This rate is suggested by typical disk masses of $0.1\,M_\odot$ around solar mass T Tau stars of 10^6 years age (e.g. Beckwith & Sargent 1993). This accretion rate is generally thought to be representative for the early stages of the evolution of a protoplanetary disc prior to the onset of planetary formation. Observationally determined mass accretion rates for young stellar objects of age less than 10^6 yr seem to (weakly) support our assumption of a mass accretion rate of $10^{-7}\,M_\odot$ yr^{-1} for the pre-planet-formation phase (e.g. Hartmann 2000). Generally the accretion rate gradually decreases with time. Therefore, for comparison also models with an accretion rate of 10^{-6} and $10^{-8}\,M_\odot\,\mathrm{yr}^{-1}$ are calculated. The former corresponds to an early evolutionary stage where the parent molecular cloud is not yet dissipated and the system is hidden behind a thick dust shell. The latter mass accretion rate probably corresponds to a late stage of the disc evolution where planet formation already is underway.

Figure 2 shows results of the model calculation for the radial variation of some important quantities defining the model structure of a disk. The full lines in the figure refer to a model with $\dot{M} = 10^{-7}\,M_\odot\,\mathrm{yr}^{-1}$ including radial drift and turbulent mixing of grains, the dashed lines show for comparison the results for the same model but radial

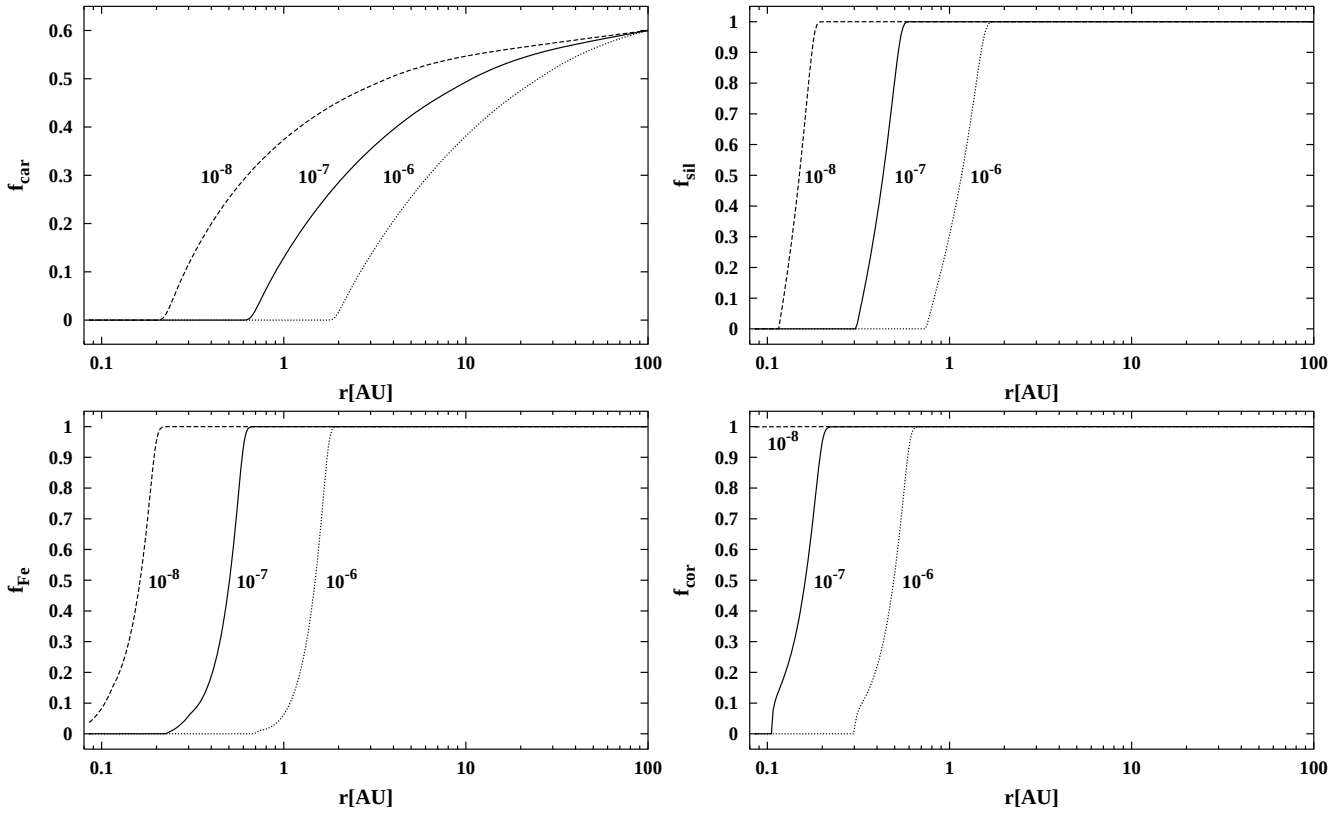

Fig. 4. Radial variation of the average degree of condensation of the key elements of the abundant dust species for three different mass accretion rates $\dot{M} = 10^{-6},\ 10^{-7},\ 10^{-8}\,M_\odot\,\mathrm{yr}^{-1}$. *Top left:* fraction of C condensed in solid carbon, *top right:* fraction of Si condensed in silicates, *bottom left:* fraction of Fe condensed in solid iron, *bottom right:* fraction of Al condensed in corundum.

mixing being neglected. In the latter case the particles are only transported inwards with the radial drift velocity v_r but there is no outwards mixing.

The main effect of radial mixing processes on the disc structure results from the following:

1. Radial mixing by diffusion transports crystalline material from the warm ($T_\mathrm{c} \gtrsim 800\,\mathrm{K}$) inner zone of the disc to quite large distances. The fraction of crystalline grains in the mixture of amorphous and crystalline grains is non-negligible up to distances of at least 10 AU (cf. Fig. 6). Since the unmodified amorphous dust from the outer disc zones, which is most likely unmodified dust from the parent molecular cloud, has a much higher mass extinction coefficient than crystalline silicate dust (cf. Fig. 1) the outward mixing of crystalline material lowers the total opacity of the dust mixture and reduces the vertical optical depth of the disc and the temperature at the midplane of the disc;
2. Radial diffusion in the disc transports material from inner disc regions with $T \gtrsim 1100\,\mathrm{K}$, where the carbon dust component is destroyed by an oxidation reaction with OH, into cool outer regions of the disc. This dilutes the carbon rich material from the outer disc regions with carbon free material from the inner disc region. As a result, the total mass extinction coefficient of the disc material is lowered as compared to when there is no mixing, since carbon dust has a high mass extinction coefficient (cf. Fig. 1) while its combustion products (CO, CH_4) have very low opacities.

The effect of radial mixing of amorphous and crystalline silicate dust, and of mixing of material with and without carbon dust, on the general disc structure represented by $\Sigma(r)$ and $h(r)$ is rather weak, it is important however for the temperature structure. In the region $0.9 \lesssim r \lesssim 10\,\mathrm{AU}$ the temperature is lower with mixing than without mixing. This effect is most pronounced in the zone between $\approx$0.9 and $\approx$3 AU.

Figure 2 also shows results for disc models with $\dot{M} = 10^{-6}$ and $10^{-7}\,M_\odot\,\mathrm{yr}^{-1}$ for comparison. The general results agree with the models for $\dot{M} = 10^{-7}\,M_\odot\,\mathrm{yr}^{-1}$, except that the disc is hotter and thicker for $\dot{M} = 10^{-6}\,M_\odot\,\mathrm{yr}^{-1}$ and is cooler and thinner for $\dot{M} = 10^{-8}\,M_\odot\,\mathrm{yr}^{-1}$.

Figure 3, left part, shows for the model with $\dot{M} = 10^{-7}\,M_\odot\,\mathrm{yr}^{-1}$ the pressure-temperature stratification in the midplane of the disc. It clearly shows some temperature plateaus which correspond to the disappearance of an important absorber. They are related to the vapourisation of water ice, iron, and corundum, and to the disappearance of amorphous in favour of crystalline silicates by annealing.

The effects of the disappearance of the various dust species can be seen from Fig. 3, right part, which shows the total extinction coefficient and the contributions of the individual dust species. Crystalline silicates are clearly

seen to be generally unimportant for the extinction of the dust material, even in the region where the amorphous dust component has disappeared by annealing. This results from the low extinction of crystalline silicates in the optical to mid-infrared spectral region. The contribution of carbon dust to the total opacity also is low in the region $\lesssim$5 AU because of the dilution of the disc material with oxidised material from the inner portions of the disc.

The consequence of this is that solid iron grains are the dominant contributors to the total opacity in the inner disc region between $\approx$1 AU and the vapourisation limit of iron (at $\approx$0.2 AU in our model) because iron is a very efficient absorber in the optical and mid-infrared region.

Figure 4 shows the radial variation of the degree of condensation f of the key elements (C for solid carbon, Si for silicates, Fe for solid iron, Al for corundum) for the four dust components considered in the model calculation.

For carbon one clearly sees the effect of mixing of oxidised material into the outer disc region which reduces the carbon abundance in regions where oxidation processes are negligibly slow and carbon is metastable against combustion. The fraction f of carbon in dust at large disc radii is 0.6 since it is assumed that a fraction of 0.4 is already present as CO molecules in the parent molecular cloud material (the Mathis-Rumpl-Nordsieck 1977 model). The carbon grains disappear in this calculation at a temperature of 1100 K. The calculation in Finocchi et al. (1997) has shown that only one half of the carbon is immediately converted into CO by the oxidation process while the other half of the carbon first forms CH_4 which is oxidised into CO at a somewhat higher temperature ($\approx$1300 K). Such gas phase processes are not considered in this paper; they will be treated in a separate paper.

For silicates, iron, and corundum Fig. 4 shows how these components disappear by vapourisation in a state of chemical equilibrium with the gas. The present calculation does not consider the radial transport of the vapour into cooler disc regions and a recondensation of this material in this zone. The variation of f is expected to be modified by such processes in the sense that the abundance of refractory elements increases in a zone near the vapourisation limit (Morfill & Völk 1984; Morfill et al. 1985). These effects will be treated in a separate paper.

6.2. Annealing of silicates

For calculating the process of annealing of amorphous silicates and the radial mixing of amorphous and crystalline silicates, we have introduced a grid of 21 discrete values of the quantity ξ between $\xi_1 = 0$ and $\xi_{21} = 1$. Figure 5 shows the results of our model calculation for the radial variation of the degree of crystallinity of the silicate grains for the model with $\dot{M} = 10^{-7}\,M_\odot\ \mathrm{yr}^{-1}$. For higher and lower accretion rates the results are similar. More precisely Fig. 5 shows the radial variation of the fraction of grains found in intervals with a degree of crystallinity between ξ^3 and

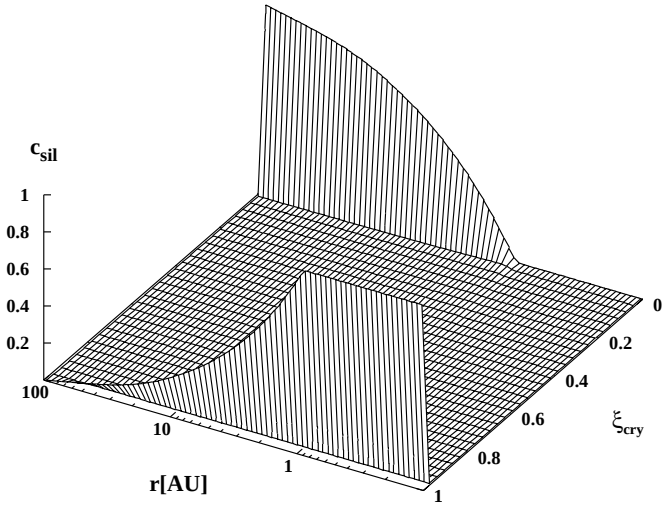

Fig. 5. Radial variation of the fraction of silicate grains with different degrees of crystallisation $0 \le \xi^3 \le 1$. The grains either are fully crystalline ($\xi = 1$) or fully amorphous ($\xi = 0$). Partially crystalline grains have only very small abundance. In the region $0.9 \lesssim r \lesssim 20$ AU one has a mixture of either fully amorphous or fully crystalline grains. Model with mass accretion rate $\dot{M} = 10^{-7}\,M_\odot\ \mathrm{yr}^{-1}$.

$(\xi_i + \Delta\xi_i)^3$ for each of the 20 intervals $[\xi_i, \xi_{i+1}]$ used in the numerical calculation.

As can be seen from Fig. 5 throughout the disc almost all grains are either completely crystalline ($\xi = 1$) or completely amorphous ($\xi = 0$). The fraction of partially crystalline grains is very small and cannot easily be seen in the figure, only as a very small hump at $r \approx 1$ AU. This results from the strong temperature dependence of the annealing process. The conversion of a completely amorphous grain into a completely crystalline grain occurs within a small temperature interval of about 30 K (see Fig. 15 in Gail 1998). Thus, a grain remains amorphous, if the temperature of the grain's environment never exceeded the critical temperature for efficient annealing to become possible ($\approx$810 K in our model) or it is rapidly annealed and becomes completely crystalline if the temperature only slightly exceeds the critical temperature. That a grain is mixed into the region where annealing starts to operate but is mixed back into a cooler zone before annealing comes to completion is a rather unlikely event. This reflects the fact that only the heating event with the highest temperature suffered by a grain contributes to the annealing (cf. Eq. (31)) and if this exceeds the temperature required for annealing then the annealing is almost certainly complete while otherwise the grain remains amorphous.

Figure 6 shows the average degree of crystallinity f_{cry} of the silicate grains calculated according to (37). This is used to calculate the opacity of the mixture of amorphous and crystalline silicate grains according to (53). In principle, f_{cry} equals the probability distribution $c(1, r)$, since grains with $0 < \xi < 1$ are rare, i.e., f_{cry} in fact is the fraction of grains being fully crystallised, the remainder

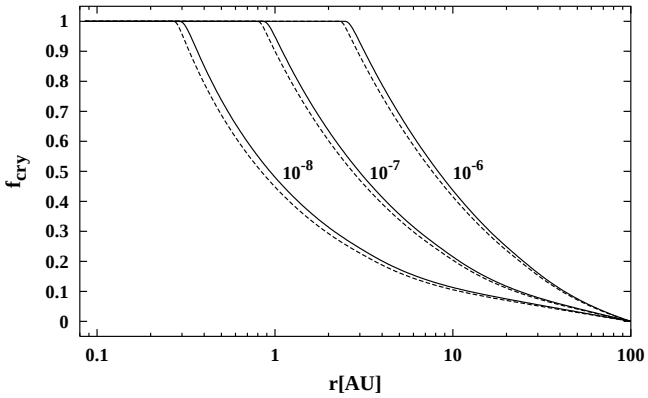

Fig. 6. Radial variation of the fraction $f_{\rm cry}$ of olivine silicate grains with a crystalline lattice structure (full line) for mass accretion rates of $\dot{M} = 10^{-6},\ 10^{-7},\ 10^{-8}\,M_\odot\,{\rm yr}^{-1}$. The quantity $f_{\rm cry}$ has only a formal meaning in the region where the silicate dust grains are vapourised. The dashed line shows the fraction of grains with crystalline lattice structure for enstatite grains for comparison.

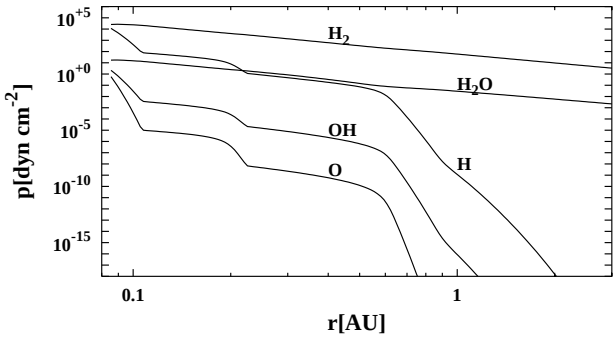

Fig. 7. Equilibrium abundance of molecules from the H-O-chemistry in the warm disc region. The step-like change of the chemical composition is due to temperature plateaus related to the disappearance of important absorbers (vapourisation of solid iron and of corundum). Model with mass accretion rate $\dot{M} = 10^{-7}\,M_\odot\,{\rm yr}^{-1}$.

fraction of the grains being fully amorphous. The numerical solution of the diffusion – transport – annealing equation formally is calculated down to the inner boundary of the disc model though at small distances from the protostar the dust is already vapourised. This is done only for computational convenience in order to avoid the introduction of a separate inner boundary for silicate dust where the boundary conditions are prescribed.

From Fig. 6 one clearly sees that a considerable fraction of crystalline dust material is present in the disc zone between 1 and more than 10 AU, where the disc is too cool to allow for the conversion of amorphous dust into crystalline dust. The high abundance of crystalline material in this region is in accord with the findings in primitive meteoritic material from the asteroidal zone of our Solar System and with the presence of crystalline silicate material in comets. This shows the importance of radial mixing for the composition of the dust material in this part of the protoplanetary disc.

For comparison Fig. 6 shows the results for the annealing of enstatite grains. Enstatite is included in the computations, but is not used for the model construction. Due to their somewhat higher activation energy for annealing the average degree of crystallinity of enstatite grains is slightly lower than that of olivine grains, the differences are, however, not really significant.

The present model calculation is based on the activation energy of annealing as determined for glassy forsterite and enstatite by Fabian et al. (2000). The results of Hallenbeck et al. (1998) and Hallenbeck et al. (2000) based on a different starting material (smokes) indicate quite a different behaviour during progressive crystallisation by annealing. Especially their results point to a higher annealing temperature of the amorphous smokes than of glassy material. From Eq. (2) of Hallenbeck et al. (2000) one calculates a characteristic annealing temperature of about 950 K where the time required to leave the "stall phase" found in the experiments equals the typical timescale of 10^4 yr for radial particle transport at 1 AU. This extends the inner boundary of existence of amorphous dust somewhat inwards compared to the results of the present model calculation for glassy material (by about 20%), but does not significantly change the results of the calculation.

6.3. Combustion of carbon grains

Figure 7 shows the variation of the abundance of free H and O atoms and of molecules of the H-O-chemistry. Of particular interest for carbon combustion is the OH abundance since surface reactions of carbon grains with this molecule are the key process for carbon dust destruction. The abundance of this radical steeply increases with increasing temperature and reaches a level sufficient for efficient carbon oxidation at about 1100 K, corresponding to a distance of 0.9 AU in our model. The step-like structure of the radial variation of the molecular abundances results from the temperature plateaus corresponding to the region where an important absorber disappears, in our case to the disappearance of solid iron and of corundum.

For calculating the process of carbon dust combustion and radial mixing, we divide the size interval between 5 nm and 0.25 μ as defined by the Mathis-Rumpl-Nordsieck (MRN) size distribution into 22 logarithmically equidistant size intervals. The initial values at the outer disk boundary for the concentration c_i of grains with radii between r_i and r_{i+1} is defined by (22) using the Mathis-Rumpl-Nordsieck (1977) size distribution. The grain size region between 0.1 and 5 nm, for which the MRN size distribution assumes that no such grains are present, is divided into seven additional size intervals for which we assume the boundary condition $c_i = 0$ at the outer disk boundary.

Figure 8 shows the result for the radial variation of the size distribution of carbon grains in the disc due to

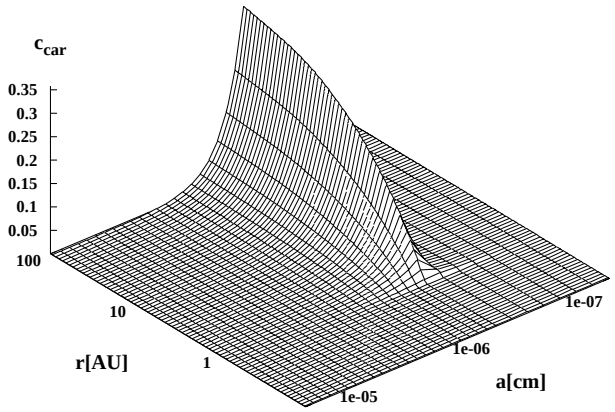

Fig. 8. Radial variation of the carbon grain size spectrum. The initial size spectrum at large distances is the Mathis-Rumpl-Nordsieck size distribution of interstellar grains. The pronounced ridge in the size distribution at a grain size of 5 nm results from the special form of the MRN size distribution. Carbon combustion at ≈1 AU removes all carbon grains from the dust mixture of the disc material. Radial mixing of the outburnt disc material dilutes the carbon dust component in the disc region between 1 and 10 AU and reduces the abundance of carbon dust. Model with mass accretion rate $\dot{M} = 10^{-7}\,M_\odot\,\mathrm{yr}^{-1}$.

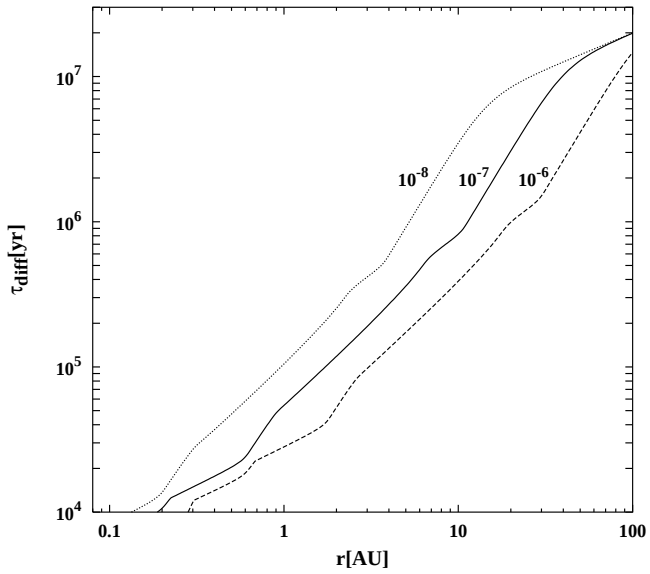

Fig. 9. Characteristic timescales for radial diffusion for the disc models with $\dot{M} = 10^{-6},\ 10^{-7},\ 10^{-8}\,M_\odot\,\mathrm{yr}^{-1}$.

radial diffusion and combustion for the model with $\dot{M} = 10^{-7}\,M_\odot\,\mathrm{yr}^{-1}$. The carbon combustion reaction is most efficient at about 1100 K where the carbon grains rapidly lose all their material by surface reactions with OH radicals. This burning temperature is solely determined by the dissociation equilibrium of the water molecules (cf. Fig. 7). Mixing of carbon free material from the disc zone with $T \gtrsim 1100$ K into cool zones of the disc reduces the abundance of dust grains in a wide region of the disc. This is most clearly seen in Fig. 4 if one compares the radial variation of f_{car} with the run of the degree of condensation of the other dust components. The reduced carbon dust abundance in the region $r \lesssim 10$ AU results in a considerable reduction of the contribution of carbon dust to the opacity of the disc material. Without consideration of the mixing process the carbon dust usually contributes roughly one half of the total opacity. If mixing is considered, the contribution of carbon dust to the opacity becomes negligible in the region $r \lesssim 10$ AU, cf. Fig. 3.

The general shape of the size distribution of carbon grains is not strongly affected by combustion and mixing in the region between $1 \lesssim r \lesssim 10$ AU, except for the general reduction of the number density and grain size. In the cold disc region we find that a small population of grains with radii less than 5 nm is build up due to mixing from the warm zone. Such grains are absent from the MRN model for the interstellar grain size distribution. However, their number density remains small. The main effect of radial mixing on the carbon dust component, especially in the disc region between 1 and 10 AU, is the mixing of carbon-dust-free material from the inner into the outer disc zones.

6.4. Validity of the stationary model

The radial mixing of dust material is calculated for the limiting case of a stationary accretion disc. In reality the disc evolves through a sequence of quasi stationary states within a region extending from roughly 0.5 to 20 AU, as may be seen from the models of Ruden & Lin (1986). Close to the star the assumption of a stationary disc breaks down because of instabilities associated with FU Ori outbursts (cf. Hartmann & Kenyon 1996) and in any case the physics of the disc is much more complicated in this region than is considered in our model calculation (e.g. Hartmann 1998). At large distances, $r \gtrsim 20$ AU, the disc never relaxes to a stationary state but slowly expands under the action of viscous torques. The present calculation can only be applied to that part of the disc which is in a nearly stationary state, i.e. to the region $r \lesssim 20$ AU.

Characteristic diffusional timescales in this region defined by the relation

$$\tau_{\mathrm{diff}} = \frac{r^2}{D} \tag{69}$$

are shown in Fig. 9. They are identical with the characteristic timescales for disc evolution. Since we are interested in an early evolutionary state of the disc prior to formation of planetary bodies, we consider disc ages less than about 10^6 years. An inspection of Fig. 9 shows that within this period material from the warm central part of the disc ($r \lesssim 1$ AU) can be mixed outwards to roughly 10...20 AU. This is approximately the region within which quasi stationary disc models can be applied. Our results for the mixing of disc material by diffusion processes are expected, thus, to be applicable within this region (this is confirmed also by time dependent models, Wehrstedt & Gail, to be published). Beyond this region the results of the present calculation are invalid because (i) in that region the disc is non-stationary and (ii) mixing beyond ≈20 AU is limited

by the slowness of the diffusion process, which is too slow to transport within the first million years of disc evolution significant amounts of material from the hot part of the disc into the outermost disc regions beyond ≈20 AU according to this model.

In the present model calculation a value of $Sc = 1$ is used for the Schmidt number. The Schmidt number relates the transport coefficients of momentum and viscosity in a turbulent flow according to (2). Laboratory results for this quantity yield values somewhat less than unity, typically of the order of 0.7 (e.g. Launder 1976; McComb 1990). We have chosen to use a value $Sc = 1$ in our calculation in order to be sure that we do not overestimate the rate of diffusional mixing. The results obtained in the present model calculation for radial mixing in the disc hence can be considered to represent a lower limit to the real extent of radial mixing taking place in a protoplanetary disc.

7. Disc spectrum

As an illustration of the consequences of mixing crystalline dust material into the outer disc region we have performed a preliminary model calculation for the infrared disc spectrum. We follow the usual concepts of LTE stellar atmosphere calculations and proceed as follows:

1) We calculate the vertical pressure stratification $P(z)$ in the upper layers of the disc between the optical depth $\tau = 10^{-6}$ and $\tau = 10$. This refers to the outer disc atmosphere where the observable disc spectrum is formed. This layer is only a small part of the total vertical extension of the disc, except in the outermost parts of the disc at large distances from the star (cf. Fig. 2).

The hydrostatic pressure equation

$$\frac{\mathrm{d}p}{\mathrm{d}z} = -\frac{GM_* z}{(r^2+z^2)^{\frac{3}{2}}}\rho \tag{70}$$

is integrated simultaneously with

$$\frac{\mathrm{d}\tau}{\mathrm{d}z} = -\kappa\rho \tag{71}$$

subject to the boundary conditions

$$p = 0\ ,\ \tau = 0 \quad \text{for } z \to \infty, \tag{72}$$

and

$$T = T_{\rm eff} \quad \text{at} \quad z = h \tag{73}$$

with h given by (41). The temperature structure $T(\tau)$ in the outer disc layer is calculated from the condition of flux constancy within the disc atmosphere (see below) and is considered to be a given quantity for this part of the calculation.

The opacity is calculated for a mixture of dust grains consisting of crystalline and amorphous olivine, carbon, iron, and corundum. At low temperatures below the vapourisation limit of water ice a coating of grains with water ice is considered.

Because the temperature decreases throughout the disc in the vertical direction the composition of the disc material varies in the vertical direction. In the innermost disc zone iron and the silicates are vapourised at the disc's midplane at $r \lesssim 0.2$ AU and corundum at $r \lesssim 0.1$ AU, but they exist as condensed solids in the disc atmosphere because $T_{\rm eff}$ exceeds the vapourisation temperature of the silicates only for $r \lesssim 0.8$ AU. Water ice exist in the region $0.9 \lesssim r \lesssim 3$ AU only in the disc atmosphere, but not at the disc's midplane. In some regions of the disc the convection currents, thus, carry material back and forth between warm and cold zones where part of the disc material is condensed or vapourised, respectively. It is assumed that vapourisation and recondensation of solids and ice occurs rapid enough compared to the timescales of convective transport that at each instant the degree of condensation of the condensible material corresponds to the degree of condensation in thermodynamic equilibrium.

With respect to carbon grains it is assumed that their size distribution is vertically constant. The change of the abundance of solid carbon grains by oxidation occurs close to the midplane, provided the midplane temperature is sufficiently high for this process to occur. The high efficiency of vertical mixing as compared to radial mixing and drift then establishes a carbon size distribution which is independent of the height z over the midplane. For the same reason we assume the degree of crystallinity of the silicates to be constant in the vertical direction.

Equations (70) and (71) are integrated simultaneously with the calculation of the equation of state, which also yields the vertical distributions of the equilibrium abundances of the minerals and water ice, which are required for calculating the dust opacity. The degree of crystallinity of the silicate dust material and the size distribution of the carbon grains are taken from the radial one zone model.

2) The radiative transfer equation is solved by the method of Feautrier (cf. Mihalas 1978). Scattering is included with the assumption of isotropic scattering. No illumination by the central star is considered, however, we do consider illumination by a 20 K warm outer molecular cloud.

The temperature structure is determined iteratively from the conditions of flux constancy and radiative equilibrium. Convective energy transport is neglected, because this energy transport mode is inefficient at the low temperatures within the disc atmosphere. The assumption of flux constancy requires that the viscous energy dissipation in the disc is concentrated in deeper layers of the disc and any contribution to the energy production from dissipation within the atmospheric region is negligible. This is satisfied for most parts of the disc except for $r \gtrsim 50$ AU where the optical depth of the disc becomes low. The temperature distribution $T(\tau)$ is then used to recalculate the vertical structure of the disc atmosphere.

The complete model is iterated by a fixed point iteration method only to an accuracy of typically 1.5%, because convergence becomes slow when the zone of disappearance by vapourisation of an important absorber, ice or silicates for instance, falls into the photosphere. The reason for this

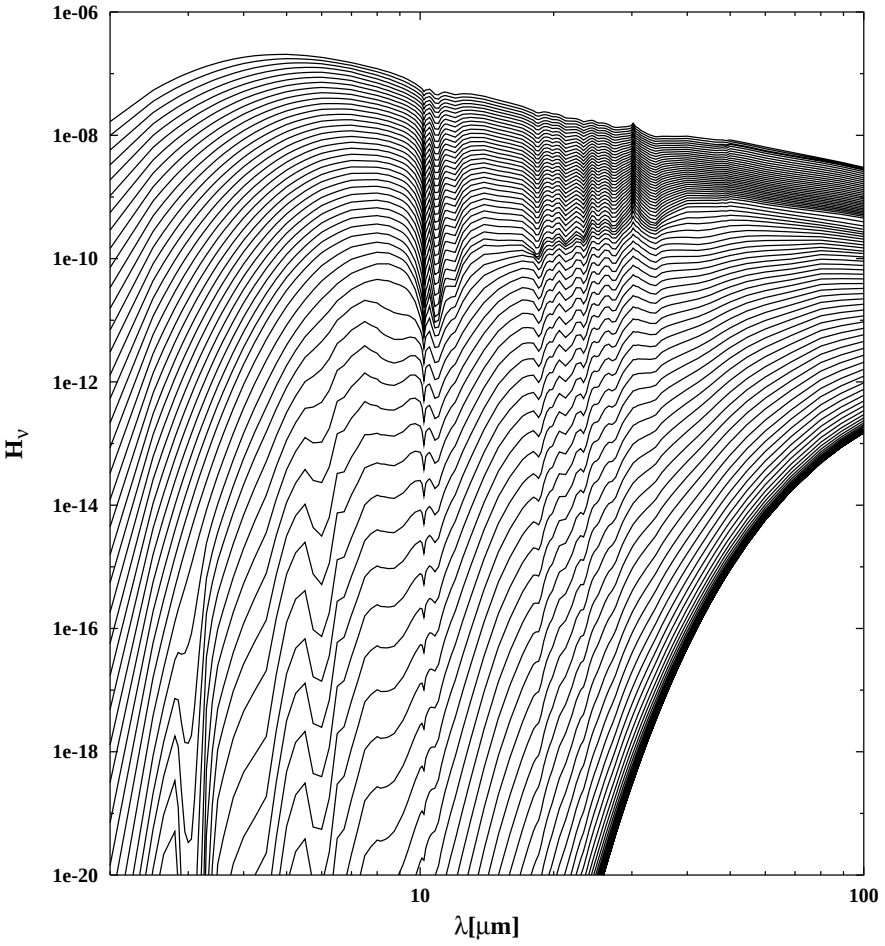

Fig. 10. Local spectra at a sequence of radii between 0.1 and 100 AU in logarithmically equidistant steps. The uppermost spectrum corresponds to the innermost radius, the lowest spectrum to the outermost radius. Clearly visible are the silicate absorption bands in the wavelength region between 8 μm and 40 μm and the ice features at $\approx$3 and $\approx$6 μm. The close spacing of the spectra at the right lower corner of the picture results from the nearly constant disc temperature in the outer regions. Model with mass accretion rate $\dot{M} = 10^{-7}\,M_\odot\,\mathrm{yr}^{-1}$.

is that small temperature changes then result in considerable opacity changes.

The local spectral energy distributions emerging from the disc surface are determined for a set of radial grid points for the model with an accretion rate of $\dot{M} = 10^{-7}\,M_\odot\,\mathrm{yr}^{-1}$.

Figure 10 shows the local disc spectra for a series of radial gridpoints between 0.1 and 100 AU. One clearly recognises the solid state absorption bands from silicate dust in the spectra. Besides the two broad absorption bands at 9.7 μm and 18 μm due to amorphous olivine, a lot of distinct and much smaller extinction features due to crystalline olivine dust superposed on the broad features of the amorphous olivine are clearly visible and additional features are seen in the 30...50 μm spectral region. A clearly visible feature around 27 μ is due to amorphous corundum. Other features of corundum are present but cannot be seen so clearly.

The features due to crystalline silicate dust are essentially limited to local disk spectra from the disc region between 1 and 10 AU where crystalline silicate dust grains either dominate or form a significant fraction of all silicate dust grains. Farther out the extinction bands of crystalline grains rapidly disappear since mixing does not carry much crystalline material beyond $\approx$10 AU during the first million years. Inside 1 AU the crystalline silicate features also

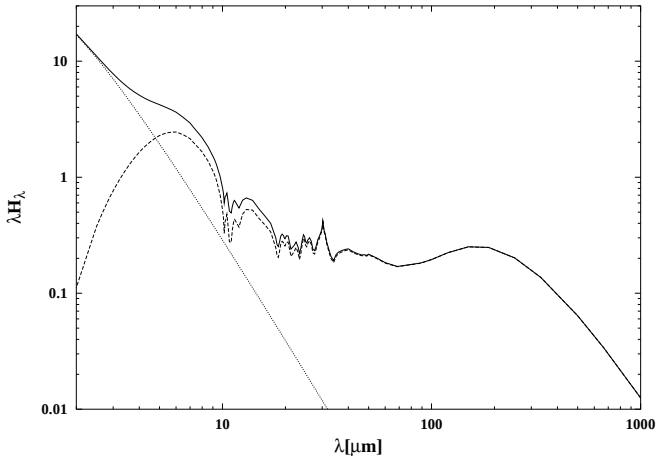

Fig. 11. Averaged disc spectrum for face-on view. Dashed line: disc spectrum. Dotted line: stellar black-body spectrum. Full line: combined spectrum. Note the spectral features due to crystalline silicate grains within the 9.7 μm and 18 μm absorption bands of the amorphous silicates and the features due to crystalline grains in the 30 to 50 μm spectral region. Model with mass accretion rate $\dot{M} = 10^{-7}\,M_\odot\,\mathrm{yr}^{-1}$.

disappear gradually with decreasing distance to the star. In this region the existence of silicate dust is confined to the disc atmosphere, because the disc becomes hot enough

to vapourise silicates throughout most of the vertical disc extension (cf. Gail 2001).

The corundum feature at 27 μm is strong in the region within $r \lesssim 1$ AU because corundum exists throughout this part of the disc even at the discs midplane, cf. Fig. 4, and is for $r \lesssim 0.2$ AU the sole solid state absorber, except in the outer layers of the disc atmosphere where additionally iron and silicates exist.

Some absorption features due to ice, especially the two at $\approx$3 μm and $\approx$6 μm are visible in the spectra from the outer disc region. Ice exists throughout the vertical extension of the disc for $r \gtrsim 5$ AU and in the outer layers of the disc atmosphere down to $r \approx 0.9$ AU. For this reason the ice features are strong in disk spectra emerging at radii $r \gtrsim 5$ AU and rapidly disappear with decreasing distance from the star and are absent from the spectra for $r \lesssim 1$ AU.

The strong concentration of the spectra in Fig. 10 for large distances results from the assumption that there is incoming radiation from a surrounding dust cloud with a temperature of 20 K.

Figure 11 shows the integrated disc spectrum for a face-on view of the disc for the set of local spectral energy distributions shown in Fig. 10. The features of the crystalline silicate grains are also clearly visible in the integrated spectrum, however the strong ice features from the outer parts of the disc cannot be seen because this part of the integrated spectrum is completely determined by radiation from the warm inner disc. Figure 11 clearly demonstrates that the crystalline dust formed by annealing at $\approx$800 K and being diffusively mixed outwards by turbulent mixing can well explain the existence of crystalline dust features seen in the ISO spectra of some protostellar accretion discs, see e.g. the spectra presented by van den Ancker (2000) and Bouwman et al. (2000).

8. Concluding remarks

We have considered the radial mixing of disc matter by turbulent diffusion in protoplanetary accretion discs. Particular emphasis was laid on two processes where it is expected, and the model calculation confirms this, that mixing of hot processed dust material into the cold outer disc zones strongly modifies the opacity of the disc material and the disc properties.

The first is destruction of the carbon dust component by oxidation, where mixing of the resulting carbon free matter into outer disc regions reduces the opacity. This process has further implications because the gaseous burning products undergo further chemical reactions in the gas phase and the resulting mixture of hydrocarbons (see Finocchi et al. 1997) and CO is mixed into outer disc regions. This aspect of the problem is not discussed in this paper since the modification of the gas phase composition does not imply any modification of the disc structure. The gas phase chemistry including radial mixing will be discussed elsewhere.

The second process treated in this paper is annealing of amorphous silicate grains, which also strongly modifies the disc properties because of the very different extinction properties of amorphous and crystalline grains. The mixing of the crystallised material into outer disc regions has not only strong implications for the disc structure but has also observational consequences for the composition of primitive meteorites and the dust component in cometary material, where it is observed that hot processed material is present despite that the parent bodies of meteorites and comets are formed in disc regions which are much too cold for annealing.

It would be premature, however, to try to compare the results of the present calculation directly to observations, because of two shortcomings of the present models.

First, we have calculated radial mixing for a stationary disc model. The diffusional mixing is, however, an intrinsically time dependent process and the extent to which material from the inner disc region is transported into outer regions depends on the time elapsed since disc formation. This holds especially for disc regions beyond $\approx$10 AU which can only be enriched with hot processed material after long periods of time. Preliminary results of time dependent model calculations for the interplay between disc evolution, annealing and carbon combustion show that the radial abundance profiles of crystalline material in the disc region $r \lesssim 10$ AU after 10^6 years of disc evolution are similar to the results for stationary discs, but are quite different in the outer disc region.

Second the present model calculation includes only two basic processes for dust destruction and dust metamorphosis, which we believe to be the two most important ones, and a rudimentary set of dust components. The real dust mix entering from the parent molecular cloud is much more complex; a possible composition is described in Pollack et al. (1994). Also the real dust mixture existing in the warm disc parts where the composition has adapted to the chemical equilibrium composition is more complicated than is considered in the present model calculation. A quantitative comparison needs to include processes as described for instance in Fegley (2000) and some additional ones in order to determine how the pristine dust mixture from the molecular cloud is converted into a chemical equilibrium mixture in the inner disc region and how the products of this dust metamorphosis are mixed outwards.

Despite of the strong simplifications of the present model calculation the results show clearly (i) that model constructions for protoplanetary discs require the inclusion of dust destruction and modification processes and of radial mixing in order to determine correctly the opacities required for the model construction and (ii) that mixing processes are important and may explain the presence of crystalline dust grains in primitive meteorites and comets.

Acknowledgements. I thank the referee J. A. Nuth for carefully reading the manuscript and for his suggestions for improving the manuscript. This work is part of a project of the

Sonderforschungsbereich 359 "Reactive flows, diffusion and transport" which is supported by the Deutsche Forschungsgemeinschaft (DFG).

References

Adams, F. C., & Lin, D. N. C. 1993, in Protostars & Planets III, ed. E. H. Levy, & J. I. Lunine (University of Arizona Press, Tucson), 721

Beckwith, S. V. W., & Sarget, A. I. 1993, in Protostars & Planets III, ed. E. H. Levy, & J. I. Lunine (University of Arizona Press, Tucson), 521

Bell, K. R., & Lin, D. N. C. 1994, ApJ, 427, 987

Bouwman, J., de Koter, A., van den Ancker, M. E., & Waters, L. B. F. M. 2000, A&A, 360, 213

Brucato, J. R., Colangeli, L., Mennella, V., Palumbo, P., & Bussoletti, E. 1999, A&A, 348, 1012

Cassen, P. 1994, Icarus, 112, 405

Cronin, J. R., Pizzarello, S., & Cruishank, D. P. 1988, in Meteorites and the early solar system, ed. J. F. Kerridge, & M. S. Matthews (University of Arizona Press, Tucson), 819

Cuzzi, J. N., Dobrovolskis, A. R., & Champney, J. M. 1993, Icarus, 106, 102

D'Alessio, P., Cantò, J., Calvet, N., & Lizano, S. 1998, ApJ, 500, 411

Drouart, A., Dubrulle, B., Gautier, D., & Robert, F. 1999, Icarus, 140, 129

Dubrulle, B. 1993, Icarus, 106, 59

Dubrulle, B., Morfill, G., & Sterzik, M. 1995, Icarus, 114, 237

Duschl, W. J., Gail, H.-P., & Tscharnuter, W. M. 1996, A&A, 312, 624

Fabian, D., Jäger, C., Henning, Th., Dorschner, J., & Mutschke, H. 2000, A&A, 364, 282

Fegley, Jr. B. 2000, Space Sci. Rev., 92, 177

Fegley, Jr. B., & Prinn, R. G. 1989, in The Formation and Evolution of Planetary Systems, ed. H. A. Weaver, & L. Danley (Cambridge University Press), 171

Finocchi, F., Gail, H.-P., & Duschl, W. J. 1997, A&A, 325, 1264

Finocchi, F., & Gail, H.-P. 1997, A&A, 327, 825

Gail, H.-P. 1998, A&A, 332, 1099

Gail, H.-P. 2001, A&A, submitted

Gail, H.-P., & Sedlmayr, E. 1999, A&A, 347, 594

Hallenbeck, S. L., Nuth III, J. A., & Daukantas, P. L. 1998, Icarus, 131, 198

Hallenbeck, S. L., Nuth, J. A., & Nelson, R. N. 2000, ApJ, 535, 247

Hanner, M. S., Hackwell, J. A., Russel, R. W., & Lynch, D. K. 1994, Icarus, 112, 490

Hartmann, L. 1998, Accretion processes in star formation (Cambridge University Press)

Hartmann, L. 2000, Space Sci. Rev., 92, 55

Hartmann, L., & Kenyon, S. J. 1996, ARA&A, 34, 207

Hirschfelder, J. O., Curtiss, C. F., & Bird, R. B. 1964, Molecular Theory of Gases and Liquids (Wiley, New York)

Launder, B. E. 1976, in Turbulence, ed. P. Bradshaw (Springer Verlag, Berlin), 231

Lenzuni, P., Gail, H.-P., & Henning, Th. 1995, ApJ, 447, 848

Lide, R. D. 1995, CRC Handbook of Chemistry and Physics, 76th ed. (CRC Press, Boca Raton etc.)

Lin, D. N. C., & Papaloizou, J. 1985, in Protostars and Planets II, ed. D. C. Black, & M. S. Matthews (Univ. of Arizona Press, Tucson), 981

Lin, D. N. C., & Papaloizou, J. C. B. 1996, ARA&A, 34, 703

Mathis, J. S., Rumpl, W., & Nordsieck, K. H. 1977, ApJ, 217, 425

McComb, W. D. 1990, The Physics of Fluid Turbulence (Oxford Science Publ.)

Mihalas, D. 1978, Stellar Atmospheres 2nd Ed. (Freeman, San Francisco)

Morfill, G. E. 1983, Icarus, 53, 41

Morfill, G. E. 1985, in Birth and Infancy of Stars, ed. R. Lucas, A. Omont, & R. Stora (Elsevier Science Publishers), 693

Morfill, G. E., & Völk, H.-J. 1984, ApJ, 287, 371

Morfill, G. E., Tscharnuter, W., & Völk, H.-J. 1985, in Protostars & Planets II, ed. D. C. Black, M. S. Matthews (University of Arizona Press, Tucson), 493

Nuth, J. A. 1999, Lunar Planet. Sci. Conf., 30, 1726

Nuth, J. A., & Donn, B. 1982, ApJ, 257, L103

Nuth, J. A., Hill, H. G. M., & Kletetschka, G. 2000, Nature, 406, 275

Papaloizou, J. C. B., & Lin, D. N. C. 1995, ARA&A, 33, 505

Pollack, J. B., Hollenbach, D., Beckwith, S., et al. 1994, ApJ, 421, 615

Pringle, J. E. 1981, ARA&A, 19, 137

Prinn, R. G. 1990, ApJ, 348, 725

Ruden, S. P., & Lin, D. N. C. 1986, ApJ, 308, 883

Ruden, S. P., & Pollack, J. B. 1991, ApJ, 375, 740

Saxena, S. K., & Eriksson, G. 1986, in Chemistry and Physics of Terrestrial Planets, ed. Saxena (Springer, New York), 30

Shakura, N. I., & Sunyaev, R. A. 1973, A&A, 24, 337

Sharp, C. M., & Huebner, W. M. 1990, ApJS, 72, 417

Shu, F. H. 1977, ApJ, 214, 448

Sogawa, H., & Kozasa, T. 1999, ApJ, 516, L33

Stahler, S. W., & Walter, F. M. 1993, in Protostars & Planets III, ed. E. H. Levy, J. I. Lunine (University of Arizona Press, Tucson), 405

Stepinski, T. F. 1998, ApJ, 507, 361

Stevenson, D. J. 1990, ApJ, 348, 730

Stevenson, D. J., & Lunine, J. I. 1988, Icarus, 75, 146

van den Ancker, M. E., Bouwman, J., Wesselius, P. R., et al. 2000, A&A, 357, 325

Waldmann, L. 1958, in Encyclopedia of Physics, Vol. XII, ed. S. Flügge (Springer, Berlin), 295

Weidenschilling, S. J., & Cuzzi, J. N. 1993, in Protostars & Planets III, ed. E. H. Levy, & J. I. Lunine (University of Arizona Press, Tucson), 1031

Wooden, D. H., Harker, D. E., Woodward, C. E., et al. 1999, ApJ, 517, 1034

Wooden, D. H., Butner, H. M., Harker, D., & Woodward, C. E. 2000, Icarus, 143, 126

Zinner, E. 1988, in Meteorites and the early solar system, ed. J. F. Kerridge, M. S. Matthews (University of Arizona Press, Tucson), 956